People's Democratic Republic of Algeria
Ministry of Higher Education and Scientific Research
Hamma Lakhdar University of El-Oued
Faculty of Technology Department
of Mechanical Engineering

THESIS

Presented with a view to obtaining the diploma of

MASTER

Sector: Electromechanical

Specialty Industrielle Maintenance

A Comparative Study of Graphical Fault Detection Methods for Power Transformers in Dissolved Gas Analysis with Artificial Intelligence Enhancements

Submitted by:
Missi Abdelhakim
Mechri Azzedine
Hachem Mabrouk

Supervised by:
Dr. Hechifa Abdelmoumene

Board of Examiners:

Dr: Laouamer Mosbah	**President**	University of El-Oued
Dr: Beggat Feteh	**Examiner**	University of El-Oued

Academic year: 2025/2026

Dedication

In the Name of Allah, the Most Gracious, the Most Merciful

I dedicate the fruit of this humble effort to:

My beloved mother — may Allah preserve her and bless her with good health and well-being — in gratitude for the love and tenderness she has always surrounded me with, and for her sincere prayers and great sacrifices that have been my support throughout every stage of my life.

To the pure soul of my late father, may Allah have mercy upon him, who was a wonderful father and mentor, and who instilled in me the values of hard work, honesty, and generosity. I pray that Allah grants him His vast mercy and the highest place in Paradise.

I also dedicate this work to my brothers, sisters, and all my beloved family members, in appreciation of their continuous support, constant encouragement, and for always standing by my side throughout this journey.

MISSI ABDELHAKIM

Dedication

In the Name of Allah, the Most Gracious, the Most Merciful

I dedicate the fruit of this humble effort to:

My beloved parents — may Allah preserve them and bless them with good health and happiness — in gratitude for their endless love, sincere prayers, and countless sacrifices, which have been my greatest source of strength and support throughout every stage of my life.

To my brothers, sisters, and all my beloved family members, in appreciation of their continuous encouragement, unwavering support, and for always standing by my side throughout this journey.

MECHRI AZZEDINNE

Dedication

In the Name of Allah, the Most Gracious, the Most Merciful

I dedicate this humble work to:

My beloved parents — may Allah preserve and protect them — in appreciation of the love and care they have always surrounded me with, the great sacrifices and efforts they have made for me, and the values of patience, perseverance, and ambition they instilled in me. They have truly been my greatest support throughout my journey.

I also dedicate this work to my brothers, sisters, and all my dear family members, in gratitude for their continuous support, sincere encouragement, and unwavering presence, which have always been a source of strength and hope for me.

HACHEM MABROUK

Absract

This study proposes an intelligent framework for power transformer fault diagnosis based on Dissolved Gas Analysis) DGA (enhanced by artificial intelligence techniques .Traditional graphical methods such as the Duval Triangle and other geometric approaches are effective but suffer from limitations related to subjectivity and inconsistency.

To overcome these challenges ,this work integrates multiple graphical DGA methods with machine learning algorithms ,including SVM, KNN ,Decision Tree , and , AdaBoost .A unified feature vector is constructed ,and SHAP-based feature selection is applied to improve interpretability and reduce dimensionality .

The results show that the proposed approach improves classification accuracy and robustness ,with ensemble models achieving the best performance . Additionally ,SHAP analysis enhances the understanding of feature importance and model decisions.

Overall ,the proposed methodology provides an accurate ,interpretable ,and efficient solution for transformer fault diagnosis and supports predictive maintenance in power systems.

Keywords :DGA ,Transformer Fault Diagnosis ,Machine Learning ,SHAP , AdaBoost

Abstract (in French)

Cette étude propose un cadre intelligent pour le diagnostic des défauts des transformateurs de puissance basé sur l'analyse des gaz dissous (DGA), améliorée par des techniques d'intelligence artificielle. Les méthodes graphiques traditionnelles telles que le triangle de Duval et d'autres approches géométriques sont efficaces, mais présentent des limites liées à la subjectivité et à l'incohérence des résultats.

Pour surmonter ces défis, ce travail intègre plusieurs méthodes graphiques DGA avec des algorithmes d'apprentissage automatique, notamment SVM, KNN, Decision Tree et AdaBoost. Un vecteur de caractéristiques unifié est construit, et une sélection de caractéristiques basée sur SHAP est appliquée afin d'améliorer l'interprétabilité et de réduire la dimensionnalité.

Les résultats montrent que l'approche proposée améliore la précision de classification et la robustesse, les modèles d'ensemble obtenant les meilleures performances. De plus, l'analyse SHAP permet une meilleure compréhension de l'importance des caractéristiques et des décisions du modèle.

Dans l'ensemble, la méthodologie proposée fournit une solution précise, interprétable et efficace pour le diagnostic des défauts des transformateurs et soutient la maintenance prédictive dans les systèmes électriques.

Mots-clés : DGA, diagnostic des défauts des transformateurs, apprentissage automatique, SHAP, AdaBoost.

Abstract (in Arabic)

الملخص

تُقترح في هذه الدراسة منظومة ذكية لتشخيص أعطال محولات القدرة الكهربائية اعتمادًا على تحليل الغازات المذابة (DGA) مع تعزيزها بتقنيات الذكاء الاصطناعي. وعلى الرغم من فعالية الطرق البيانية التقليدية مثل مثلث دوفال وغيرها من الأساليب الهندسية، إلا أنها تعاني من محدودية تتمثل في الذاتية وعدم الاتساق في نتائج التشخيص.

لمعالجة هذه الإشكاليات، تم دمج عدة طرق بيانية لتحليل DGA مع خوارزميات تعلم الآلة مثل SVM وKNN وDecision Tree وAdaBoost، وذلك ضمن إطار موحد يعتمد على متجه ميزات شامل. كما تم تطبيق اختيار الميزات باستخدام SHAP بهدف تحسين قابلية التفسير وتقليل الأبعاد مع الحفاظ على المعلومات الأكثر تأثيرًا في عملية التصنيف.

أظهرت النتائج أن المنهج المقترح يحقق تحسنًا واضحًا في دقة التصنيف وموثوقية النماذج، حيث سجلت النماذج التجميعية (Ensemble) أفضل أداء مقارنة ببقية الخوارزميات. بالإضافة إلى ذلك، ساهم تحليل SHAP في توضيح تأثير كل ميزة على قرارات النموذج، مما عزز من شفافية النظام.

بشكل عام، يوفر هذا العمل إطارًا فعالًا ودقيقًا وقابلًا للتفسير لتشخيص أعطال المحولات، ويدعم تطبيقات الصيانة التنبؤية في أنظمة القدرة الكهربائية.

الكلمات المفتاحية: تحليل الغازات المذابة (DGA)، تشخيص أعطال المحولات، تعلم الآلة، SHAP، AdaBoost.

Table of Contents

List of Figures

List of Figures

List of Tables

Acronym

DGA	Dissolved Gas Analysis
IEC	International Electrotechnical Commission
PD	Partial Discharge
D1	Low Energy Discharges
D2	High Energy Discharges
T1	Faults (<300°C)
T2	Faults (300°C-700°C)
T3	Faults (>700°C)
FRA	Frequency Response Analysis
IFT	Interfacial Tension
IR	Insulation Resistance
DP	Degree Of Polymerization
DPC	Polarization And Depolarization Current
BDV	Breakdown Voltage
RVM	Recovery Voltage Measurement
HST	Hot Spot Temperature
GC	Gas Chromatography
RL	Reinforcement Learning
TRT	Three Ratio Technique
DTM	Duval Triangle Method
DPM	Duval Pentagon Method
MPM	Mansour Pentagon Method
GTM	Gouda Triangle Method
RFRM	Rogers' Four Ratios Method
AI	Artificial Intelligence
ML	Machine Learning
DL	Deep Learning

GBT	Gradient Boosted Tree
PCA	Principal Component Analysis
MBC	Maximum Boost Control
LSTM	Long Short-Term Memory
DT	Decision Trees
SVM	Support Vector Machine
KNN	K Nearest Neighbor
RBFN	Radial Basis Function Networks
GWO	Gray Wolf Optimization
WOA	Whale Optimization Algorithm

Introduction

Introduction

Electric power transformers are essential components of electrical power systems, ensuring the efficient and safe transmission and distribution of electrical energy by maintaining appropriate voltage levels to meet consumer demands. With continuous technological advancement and increasing load demands on power networks, transformer failures have become more significant, both operationally and economically. Consequently, the development of accurate and reliable diagnostic techniques has become a critical requirement. [1]

One of the most widely used traditional techniques for diagnosing transformer faults is Dissolved Gas Analysis (DGA) of transformer oil. This method enables early detection of thermal, electrical, and mechanical faults by identifying and analyzing gases generated due to insulation degradation or abnormal operating conditions. Despite its effectiveness, DGA relies heavily on expert interpretation, which may lead to inconsistent diagnoses, subjective decisions, and delays in maintenance actions. [2]

In recent years, **artificial intelligence (AI) and machine learning (ML) techniques** have emerged as powerful tools for improving the accuracy of transformer fault diagnosis. These approaches facilitate the analysis of large datasets, reduce dependence on human expertise, and enable more precise fault classification and early prediction compared to conventional diagnostic methods.

Motivated by these advancements, the present research aims to **integrate Dissolved Gas Analysis (DGA) with AI/ML techniques** to develop an intelligent diagnostic model capable of supporting **preventive maintenance** and enabling **early fault detection** in power transformers. [3]

Although Dissolved Gas Analysis (DGA) provides valuable information about transformer condition, exclusive reliance on traditional diagnostic and graphical methods may result in inaccuracies due to several limitations:

- Variations in expert interpretation of DGA results
- Limited capability of traditional methods to effectively handle large datasets
- Inconsistencies between different graphical diagnostic techniques
- Difficulty in detecting and predicting complex or combined faults at an early stage

These limitations reduce the reliability and consistency of fault diagnosis, especially in modern power systems where large volumes of data and complex fault patterns are increasingly common.

Accordingly, the main research question of this study is:

How can the accuracy and consistency of power transformer fault diagnosis be improved through a comparative analysis of graphical DGA methods enhanced by artificial intelligence techniques?

The research presented in this thesis contributes to the development of an advanced and intelligent framework for assessing the condition of power transformers based on Dissolved Gas Analysis (DGA). The main contributions of this work are summarized as follows:

- A comparative framework for evaluating different graphical fault detection methods in DGA has been developed. This framework analyzes the performance of various graphical method vectors and identifies the most suitable techniques for accurate fault diagnosis.
- A fault diagnosis model based on tree-based ensemble learning algorithms has been proposed. This model integrates information derived from multiple graphical DGA methods, allowing for improved classification accuracy and more consistent diagnostic results.
- A novel hybrid approach combining machine learning and ensemble techniques has been introduced. This approach exploits the essential features extracted from graphical DGA methods to enhance fault detection capabilities.
- A data augmentation strategy based on deep learning techniques has been implemented to generate synthetic DGA data. This contribution addresses the limitation of insufficient publicly available datasets and improves the robustness and generalization of the proposed models.

These contributions collectively enhance the reliability, accuracy, and consistency of transformer fault diagnosis, while reducing dependence on subjective expert interpretation.

The main objectives of this research are as follows:

- To present the fundamentals of power transformers, including their main components and common fault types
- To review traditional graphical fault detection methods based on Dissolved Gas Analysis (DGA), highlighting their principles, advantages, and limitations
- To perform a comparative analysis of different graphical DGA methods in terms of accuracy, consistency, and diagnostic capability
- To apply artificial intelligence and machine learning techniques to DGA data for improved fault classification and pattern recognition
- To develop an intelligent diagnostic model that integrates graphical methods with AI techniques for enhanced fault detection
- To evaluate and compare the performance of traditional graphical methods and AI-based approaches in order to determine their effectiveness in improving diagnostic accuracy and reliability.

This thesis is organized into four main chapters, each building upon the previous to provide a comprehensive framework for transformer fault diagnosis:

Chapter One: Power Transformers

This chapter introduces power transformers, including their definition, operating principles, and main components. It also provides an overview of common fault types, their causes, and the operational and economic impacts of transformer failures. This foundation prepares the reader for understanding diagnostic techniques in subsequent chapters.

Chapter Two: Dissolved Gas Analysis and Graphical Fault Detection Methods

This chapter focuses on Dissolved Gas Analysis (DGA) as a key technique for transformer condition monitoring. Special emphasis is placed on graphical fault detection methods, reviewing their principles, advantages, and limitations. The chapter highlights challenges and inconsistencies in traditional graphical methods, providing motivation for AI-based enhancements.

Chapter Three: Artificial Intelligence Techniques for Fault Diagnosis

This chapter presents the proposed methodology, integrating graphical DGA methods with AI and machine learning techniques. It covers model development, feature extraction, hybrid ensemble approaches, and synthetic data generation to address limited datasets. The chapter also explains how these AI-enhanced methods aim to improve diagnostic accuracy, consistency, and early fault detection.

Chapter Four: Application and Evaluation of AI Techniques

This chapter presents the practical implementation of the proposed AI models on real and synthetic DGA datasets. It evaluates the performance of AI-enhanced methods against traditional graphical approaches using metrics such as accuracy, precision, recall, and F1-score. Comparative analysis and discussion of results highlight improvements in fault detection, consistency, and early prediction, along with practical recommendations for transformer maintenance strategies.

Conclusion

The thesis concludes with a summary of key findings, emphasizing the effectiveness of integrating graphical DGA methods with AI techniques. It discusses the impact on diagnostic reliability, preventive maintenance, and proposes directions for future research, including dataset expansion, refinement of AI models, and exploration of additional diagnostic features.

Chapter I Power Transformer

I.1 Introduction

Power transformers are among the most fundamental components of modern electrical power systems, as they play a crucial role in the efficient and secure transmission and distribution of electrical energy across different voltage levels. Transformer operation is based on the principle of electromagnetic induction, which allows electrical energy to be transferred from one voltage level to another without altering the frequency, while minimizing energy losses to the greatest extent possible.

Power transformers differ in their size, capacity, and field of application. They include small distribution transformers designed to supply end users, medium-rated transformers used for interconnecting secondary networks, and large-scale transformers employed in power generation plants and high-voltage transmission systems. The selection of an appropriate transformer depends on several factors, including the required power rating, primary and secondary voltage levels, and the characteristics of the electrical network.

A thorough understanding of transformer characteristics, types, and practical significance is essential for ensuring the reliability and stability of electrical power systems and for reducing energy losses. Consequently, power transformers represent a core subject in the field of electrical and power engineering [4].

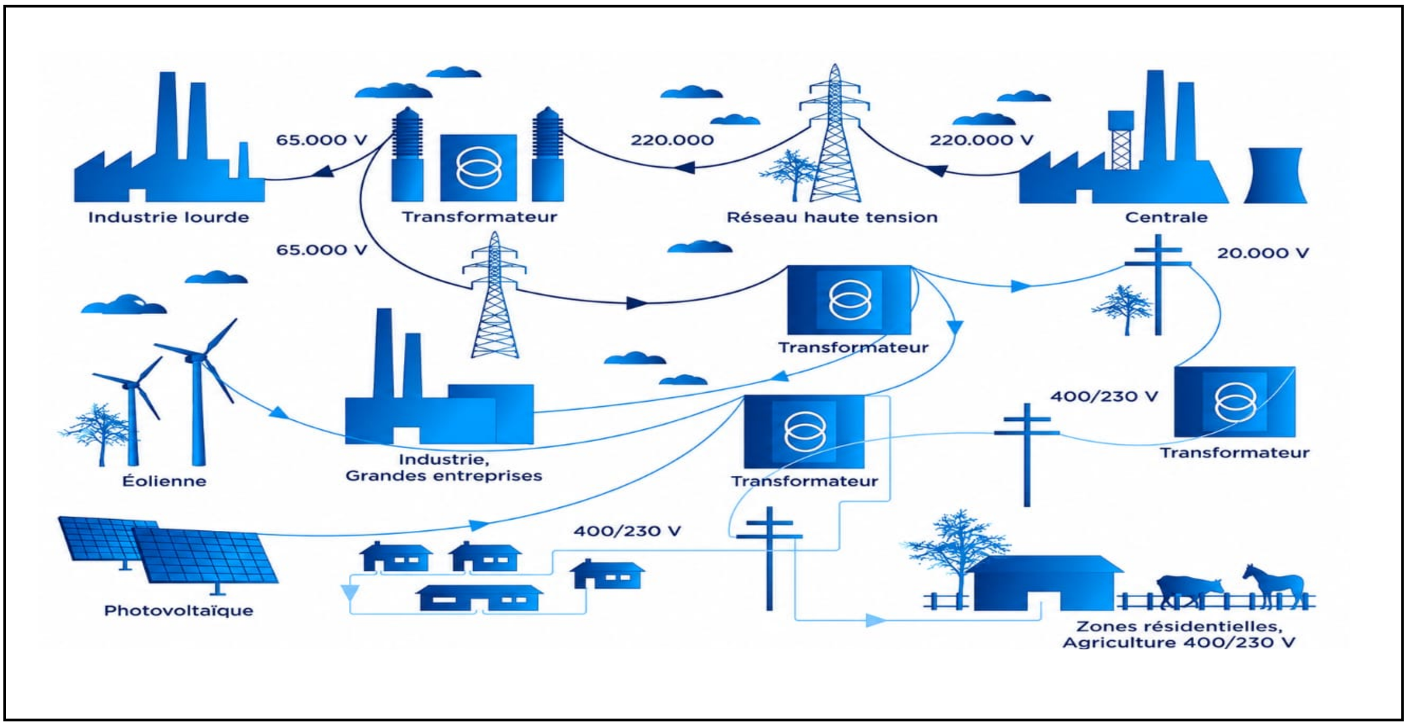

Figure I.1 transformers in the electrical power network[4].

Figure (I.1) shows the strategic position of power transformers within electric power transmission and distribution networks. In any given substation, these transformers account for approximately 60% of the investment capital, making it essential that they operate correctly and reliably for many years.

A power transformer is a high-voltage electrical component essential for the operation of electrical networks. According to the International Electrotechnical Commission (IEC), it is defined as: "A static device with two or more windings that, by electromagnetic induction, converts an alternating voltage and current system into another voltage and current system, generally of different values, at the same frequency, for the purpose of transmitting electrical power."

A transformer can be single-phase or three-phase and can employ various connection configurations: star (wye), delta, or zigzag.

This chapter provides a brief overview of transformers, their types, and components, with a focus on the insulation system, as the transformer's lifespan strongly depends on the condition of its insulation, and most condition assessment tests are conducted on it.

I.2 Power transformer:

An electric transformer is a static electrical device used in power systems to convert alternating voltage and current from one level to another (step-up or step-down) while maintaining the same frequency, based on the principle of electromagnetic induction.

Transformers are primarily used for the efficient transmission and distribution of electrical energy, allowing voltage to be increased to reduce energy losses during transmission, and then decreased to levels suitable for industrial or residential use [5].

Figure I.2 A power transformer in an electrical substation [5].

I.2.1 Operating Principle of an Electric Transformer

The operating principle of an electric transformer is based on the phenomenon of electromagnetic induction, discovered by Faraday. When the primary w

inding of the transformer is supplied with an alternating current, a time-varying magnetic flux is generated within the magnetic core. This magnetic flux is transferred through the core and links the turns of the secondary winding, inducing an electromotive force (EMF) in the secondary winding.

The magnitude of the induced voltage in the secondary winding is directly proportional to the number of its turns relative to the number of turns in the primary winding, according to the voltage transformation ratio. In this way, a transformer can step up or step down the voltage without changing the frequency. There is no direct electrical connection between the primary and secondary circuits; instead, energy transfer occurs solely through the magnetic field.

This principle is widely applied in electrical power transmission and distribution networks, where voltage is increased during transmission to reduce power losses and then decreased to levels suitable for industrial or residential consumption [6].

I.2.2 Main Components of a Power Transformer

A power transformer consists of several essential components that work together to ensure the efficient and safe transfer of electrical energy.

- ✓ **Active part:**

The magnetic core is made of laminated silicon steel sheets to reduce losses.

The primary winding generates an alternating magnetic field when connected to the power supply.

The secondary winding produces the output voltage (step-up or step-down depending on the number of turns).

- ✓ **Insulation system:**

Separates the windings from each other and from the core to prevent short circuits.

Usually consists of transformer oil, insulating paper, and other insulating materials.

- **Transformer oil:**

Acts as electrical insulation.

- Helps dissipate heat inside the transformer.

- **Metallic tank:**

Protects internal components from external effects.

Contributes to heat dissipation.

- **Radiators:**

Improve cooling by transferring heat from the oil to the surrounding air.

- **Tap changer:**

Regulates output voltage by changing the winding turns ratio according to load conditions.

- **Insulated bushings:**

Allow electrical conductors to pass safely through the tank while maintaining insulation.

- **Protection and monitoring devices:**

Include Buchholz relay, temperature indicators, and pressure relief valves.
Detect abnormal operating conditions and protect the transformer from faults [7]

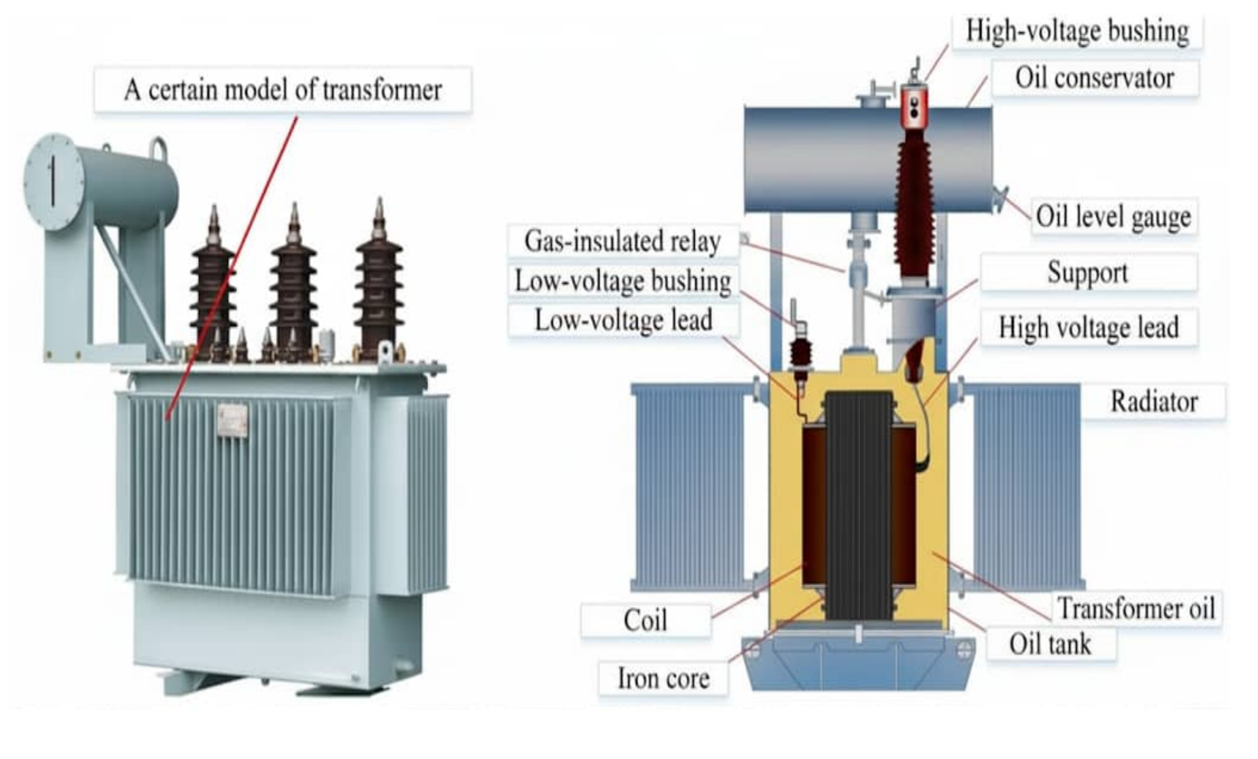

Figure I.3 Schematic Diagram of a Power Transformer [7].

I.2.3 Types of Transformers

The International Electrotechnical Commission (IEC) classifies oil-immersed power transformers into three categories based on their apparent power capacity:

• **Distribution transformer:** up to 2,500 kVA for three-phase and 833 kVA for single-phase transformers.

• **Medium power transformer:** ranging from 2.5 MVA to 100 MVA for three-phase and 33.3 MVA for single-phase transformers.

• Large **power transformer:** above 100 MVA for three-phase and above 33.3 MVA for single-phase transformers [8].

I.3 Incipient faults classification in power transformers

Power transformers can experience faults due to electrical, thermal, or mechanical stresses during normal operation. Although the occurrence of stress-related faults is generally low and remains stable for most of the transformer's life, they are important because early signs can often be detected before a complete failure occurs. The main types of faults are described below:

I.3.1 Electrical Faults

Electrical faults happen when current flows between points that are normally insulated. They can also arise from short circuits in transformer windings or loose connections. These faults are categorized based on the energy involved: high-energy discharges (D2) and low-energy discharges (D1). Discharges can damage solid insulation and create carbon particles in the oil, and as the energy increases, gas alarms may trigger and equipment failure can occur.

I.3.2 Partial Discharge

Partial discharge occurs when the insulation between conductors is not fully effective. A common type is corona discharge, which usually appears in the gaseous medium around conductors, away from solid or liquid insulation. PD does not create a low-resistance path for high currents but can still affect transformer performance, often going unnoticed until a fault develops. Its effects become significant at several thousand volts and may increase noise in sensitive equipment. Detection methods exist but are mostly qualitative and provide limited guidance for acceptable limits due to variations in voltage and insulation types.

I.3.3 Thermal Faults

Thermal faults result from overheating that produces localized hot spots in the insulation. They are classified by temperature: T1 (<300°C), T2 (300–700°C), and T3 (>700°C). Causes include poor connections, circulating currents, or magnetic flux leakage. Thermal faults raise the transformer oil temperature and generate more gases than electrical faults for the same duration. The type and amount of gases vary with temperature, making them useful for fault diagnosis [9] .

I.4 Effect of Insulation and Oil in Power Transformers

I.4.1 Insulation Effects

Electrical insulation (whether paper, plastic, or resin-based) is used to separate the windings from each other and from the magnetic core, preventing short circuits or current leakage.

Effects on the Transformer:

- ✓ **Prevention of electrical faults:** Reduces the likelihood of sparking or electrical arcing between windings.
- ✓ **Extended transformer life:** The better and more durable the insulation, the longer the transformer can operate without faults.
- ✓ **Reduced losses:** Good insulation prevents current leakage to other parts of the transformer, thereby minimizing electrical losses.

- ✓ **Impact on operating voltage:** Weak insulation limits the transformer's ability to withstand high voltages and increases the risk of breakdown.

I.4.2 Oil Effects

Transformer oil serves more than just a cooling purpose; it has two main functions:

- ✓ **Electrical insulation:** Prevents arcing between windings or between the windings and the tank.
- ✓ **Cooling:** Transfers heat generated during operation to the transformer surface, where it is dissipated into the air or via radiators.

Effects on the Transformer:

- ✓ **Increased voltage withstand capability:** Good oil prevents partial discharges or sparking under high voltage.
- ✓ **Protection of insulation:** Oil protects the insulating paper from moisture and oxidation, helping maintain insulation strength for a longer period.
  - ✓ **Improved thermal efficiency:** The transformer operates at lower temperatures, reducing losses caused by the resistance of the windings.
  - ✓ **Transformer safety:** Any oil shortage or contamination increases the risk of electrical breakdown and, in extreme cases, may cause transformer fire [10].

I.5 Conclusion

Power transformers are vital components in modern electrical networks, enabling efficient and safe voltage conversion across different levels. They consist of key parts such as the active core, insulation system, transformer oil, tank, radiators, tap changer, bushings, and protection devices, all ensuring reliable operation. Insulation and oil play a major role in reducing losses and extending transformer life. Despite careful design, transformers can experience electrical, thermal, or mechanical faults, which will be studied in detail in the next chapter.

Chapter II Dissolved Gas Analysis (DGA)

II.1 Introduction

Dissolved Gas Analysis (DGA) is considered one of the most important diagnostic methods for monitoring the condition of electrical transformers. It relies on studying the gases produced from the decomposition of the internal insulation, particularly the insulating oil, when exposed to electrical or thermal stress. The primary goal of this analysis is to detect potential faults at an early stage, such as partial discharge, excessive heat, and chemical decomposition of the oil and paper insulation, before these faults develop into serious problems that could lead to transformer failure. DGA is an effective tool for assessing the operational condition of a transformer, assisting in planning preventive maintenance, and reducing the economic risks associated with unexpected failures, making it a global standard in transformer maintenance [11]. This chapter covers the fundamental principles of dissolved gas analysis, the various methods for testing oils and extracting gases, as well as interpreting the results and correlating them with potential faults, highlighting the importance of DGA in enhancing the reliability of electrical networks and ensuring their continuous operation efficiently and safely.

II.2 Comprehensive Review of Transformer Condition Monitoring Methods

Maintenance and monitoring of transformers have important roles in the energy and system management, where the condition of transformers plays an effective role in the transmission of electricity and energy, and any malfunction in the transformer would affect the entire network [12]. Among the methods for evaluating the condition of a transformer, frequency response analysis (FRA), or as it is called, the transfer function method, is an effective method for identifying mechanical faults, including winding deformation [13-15]. PD analysis is also used for monitor power transformer. PD method is a discharge of electrical insulation, whether liquid or solid, where early detection of partial discharge reduces aging and extends the life of the transformer [16-18]. Alongside, these two methods we find vibration analysis. Vibration is usually the result of a mechanical movement, and this explains the use of vibration analysis to detect mechanical faults such as looseness, imbalance, misalignment [19, 20]. This method is not limited to mechanical systems only, but in recent years vibration analysis is used to monitor power transformer [21]. Interfacial tension (IFT) is other method. It is a chemical analysis test for the detection of acidic contaminants in oil as a result of the oxidative decomposition of paper [22, 23].Insulation resistance (IR) is to evaluate the insulation deterioration in the windings, based on the insulation resistance test, where the Polarization Index helps in reading the insulation resistance information [24].Thermography analysis is a significant method using a thermal imaging camera to detect hot spot temperature (HST) in infrared. Red and white colors represent hot areas and blue and black colors represent cold areas [25-27].Degree of polymerization (DP) is a useful way to increase the reliability of paper insulation, as the mechanical strength of the paper depends on the cellulose particles and their good bonding [28, 29].Polarization and Depolarization Current (PDC) is a time analysis for evaluating high-voltage insulation as it has the ability to determine the moisture value of oil and paper insulation and reduce deterioration [30, 31].Breakdown voltage (BDV) is as per IEC 60156 standard that the dielectric strength of the oil is determined by measuring the breakdown voltage and is conducted at room temperatures [32, 33].Recovery voltage measurement (RVM) is considered an indicator of the deterioration of the insulation, and although it is an old method, it is an effective method in determining the condition of the oil insulation [34-36].Voltage and current measurements are a method that depends on the voltage difference and the correlation between the incoming and outgoing current. To know the extent of the different types and severity of faults, simulation, experimentation and the online detection must be done [37-39].

Finally, dissolved gas analysis method (DGA) is the best technique in determining the state of a transformer over the ages, owing to its significance in diagnosing faults in oil-filled transformers and is considered a continuous study because it always seeks to develop methods for interpreting the method of DGA [40], whether by traditional methods, new and old, or by using artificial intelligence (AI). Figure II.2 presents methods for evaluating power transformers and methods for interpreting DGA in particular.

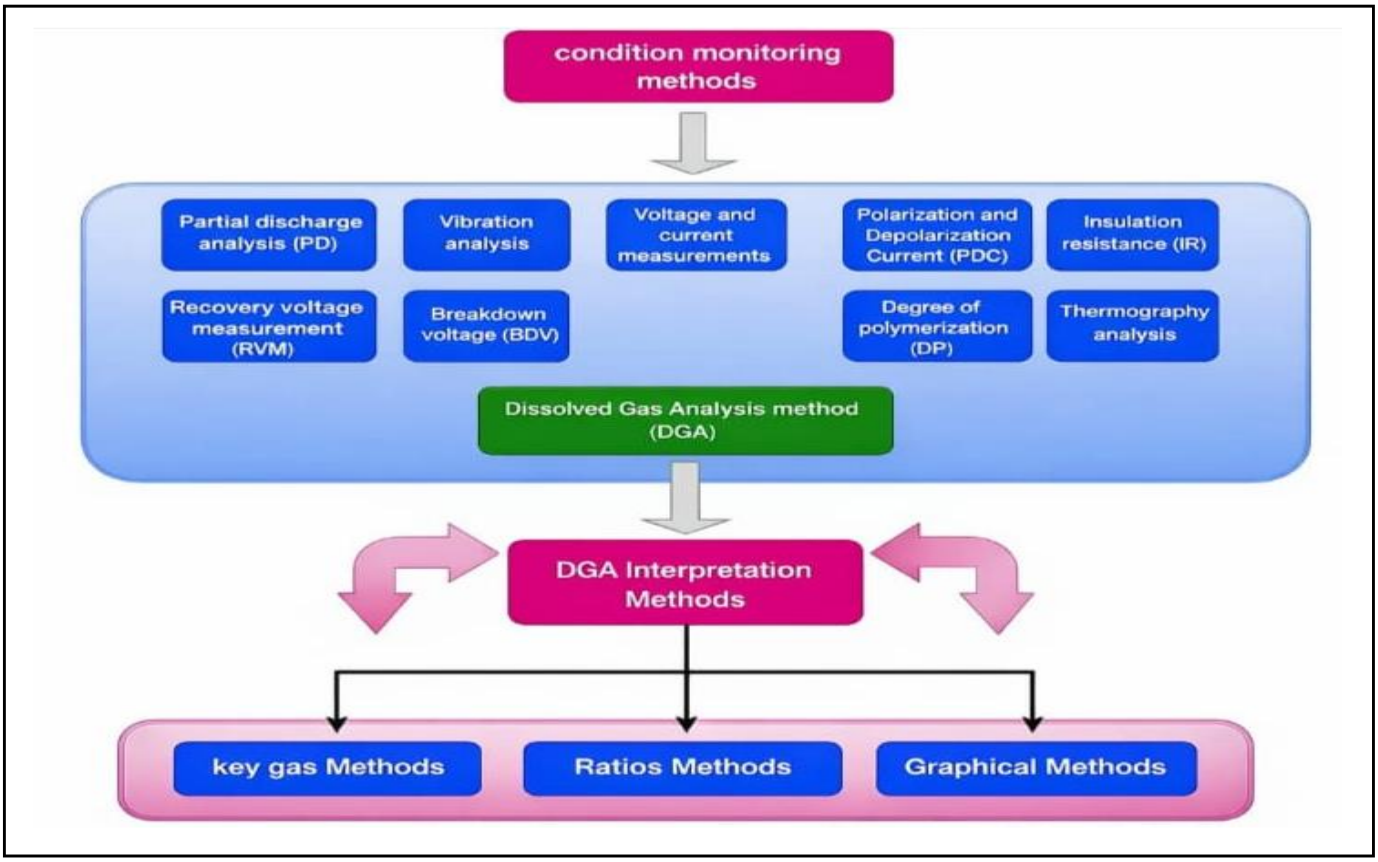

Figure II.1 Power transformer condition assessment and DGA interpretation methods

II.3 Dissolved Gas Analysis (DGA) Techniques

Dissolved Gas Analysis (DGA) is recognized as one of the most effective diagnostic approaches for identifying early-stage faults in oil-immersed power transformers[41]. This technique is based on examining the gases dissolved in transformer insulating oil, which are generated as a result of thermal, electrical, or mechanical stresses that compromise transformer performance and reliability. The analysis of these gases provides valuab le insight into the internal condition of the transformer. [42-43]

The principal gases typically monitored in DGA include hydrogen (H_2), methane (CH_4), ethane (C_2H_6), ethylene (C_2H_4), and acetylene (C_2H_2), each of which is associated with specific fault mechanisms. Furthermore, the degradation of cellulose-based insulation materials leads to the formation of carbon monoxide (CO) and carbon dioxide (CO_2), which serve as key indicators of paper insulation deterioration. [44-45]

One of the earliest protective devices associated with gas formation in transformers is the Buchholz relay, introduced in 1928 [46]. This relay operates by detecting gas accumulation caused by internal faults within the transformer. Installed in the pipeline between the main tank and the conservator, the relay responds to gas flow or oil movement, initiating an alarm or triggering a circuit breaker to isolate the transformer and prevent further damage.

With advancements in analytical methods during the late 1950s, more precise techniques for gas detection and analysis were developed. In1959 [47], H. H. Wagner introduced a gas chromatography-based analyser, marking a significant milestone in transformer diagnostics. Gas chromatography (GC) has since become the most widely

Adopted technique for the qualitative and quantitative assessment of dissolved gases, particularly those generated by electrical faults [48].

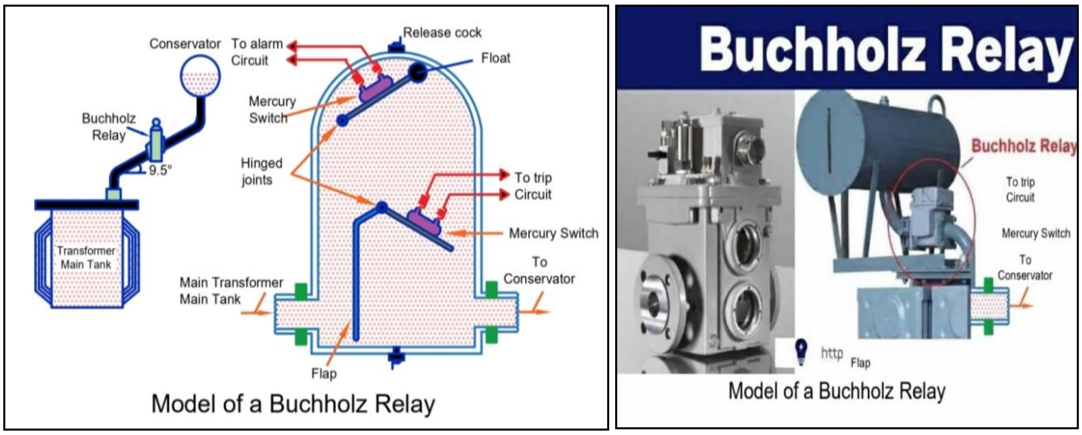

(a) (b)

Figure II.2 Buchholz relay, (a) electrical schematic; (b) an example of a Buchholz relay

The analysis of dissolved gases in oil by gas chromatography involves several key steps. The process begins with sampling, using flexible aluminum bottles or a syringe, with the option to temporarily store gases in the Buchholz relay [49]. Subsequently, the gases are extracted and analyzed using a **gas chromatograph**, which separates and quantifies them [50]. **Figure II.3** illustrates the sequential process from sample collection to analysis, ensuring accurate diagnostics and supporting preventive maintenance to avoid transformer failures.

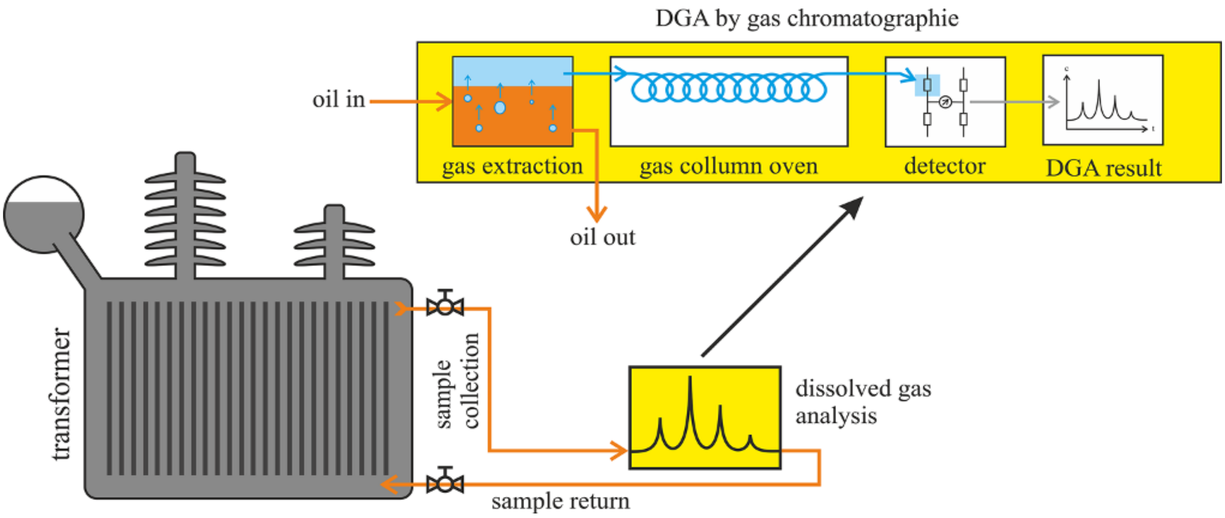

Figure II.3 Steps for gas chromatography analysis [51]

II.4 Commonly Used DGA Diagnostic Methods

This section presents an overview of the most widely applied DGA interpretation techniques, focusing on methods that have demonstrated high reliability and accuracy in practical applications. These approaches have gained broad acceptance within the power industry due to their effectiveness in assessing transformer health and diagnosing fault conditions.

II.4.1 Key Gas Methods

II.4.1.1 IEEE Key Gas Method

The IEEE Key Gas method, originally conceptualized in 1973 by the Doble Engineering Company, forms the basis for assessing power transformer conditions through the analysis of gas composition resulting from thermal and electrical stresses. This diagnostic technique was first introduced by David Pugh in 1974 [52], and its refined version was later incorporated into the Standard IEEE C57.104. This method employs the concentrations of specific gases, including hydrogen, hydrocarbons, and carbon monoxide, generated during the decomposition of both oil and paper. Table II.1 outlines the principal gases utilized alongside their associated faults, while Table II.2 details the gas ratios corresponding to the 4 main fault types identified through this method. The percentages referenced in Table II.1 and Table II.2 are based on the empirical observations of numerous experts in the field [53]. However, the IEEE Key Gas method is not without limitations; it can sometimes produce ambiguous or incorrect diagnoses. Additionally, in some cases, the dominant gas detected is not one of the primary gases considered by this method, and carbon monoxide is mistakenly interpreted as an indication that paper insulation is involved in the malfunction [54].

Table II.1 Key gas generated according to a fault type [53]

Key gas	Fault type	Typical proportions
C_2H_4	Overheating, oil	Mainly C_2H_4; Smaller proportions of C_2H_6, CH_4, and H_2; Traces of C_2H_2 at very high fault temperature
CO	Overheating, paper and oil	Mainly CO; Much smaller quantities of hydrocarbon gases (Predominantly C_2H_4 with smaller proportions of C_2H_6, CH_4, and H_2)
H_2	Partial discharge	Mainly H_2; Small quantities of CH_4; Traces of C_2H_4 and C_2H_6
H_2& C_2H_2	Arcing	Mainly H_2 and C_2H_2; Minor traces of CH_4, C_2H_4, and C_2H_6; Also, CO if cellulose is involved

Table II.2 Key gas proportions of fault types of IEEE key gas method [54]

	Key gas percentages (%)					
Fault type	**H_2**	**CH_4**	**C_2H_6**	**C_2H_4**	**C_2H_2**	**CO**
Partial discharges	85	13	1	1	-	-
Arcing	60	5	2	3	30	-
Overheating, oil	2	16	19	63	-	-
Overheating, paper	-	-	-	-	-	92

II.4.1.2 CSUS Key Gas Method

The CSUS Key Gas method, also referred to as the Key Gas Quantity Method, was developed through a collaboration between California State University, Sacramento, and the Pacific Gas and Electric Company (PG&E) [55]. This method evaluates the concentrations of hydrocarbon and carbonaceous gases independently, comparing them with the specified threshold values for each gas. Table II.3 presents both standard and non-standard limits for each gas, enabling a more accurate diagnosis of transformer faults.

Table II.3 Determination of the type of fault according to the CSUS method [55]

Key gas	Limit concentrations: Normal	Limit concentrations: Anormal	Fault type
H_2	150	1000	Corona discharges, arcing
CH_4	25	80	Corona discharges
C_2H_6	10	35	Local overheating
C_2H_4	20	150	Severe overheating
C_2H_2	15	70	Arcing
CO	500	1000	Overload, paper decomposition
CO_2	10 000	15 000	Overload, paper decomposition

When the measured concentrations of all dissolved gases remain below their prescribed normal thresholds, the transformer is regarded as operating under acceptable conditions. The identification of possible fault types is carried out by evaluating each gas concentration separately in relation to its corresponding limit. Nevertheless, although the CSUS Key Gas method is easy to apply and interpret, its diagnostic reliability is limited, as it may lead to ambiguous results by suggesting the presence of more than one fault at the same time.

II.4.1.3 CIGRE Key Gas Method

The CIGRE Key Gas method involves directly comparing the measured levels of key gases with their allowed thresholds. Introduced by CIGRE Task Force 15.01.01 [56], this method goes beyond the traditional three main fault types by also detecting faults associated with paper insulation deterioration. Table II.4 lists typical threshold values for the key gases, along with the types of malfunctions that may occur if these limits are exceeded. While this method offers useful diagnostic information, it is seldom applied on its own for assessing transformer condition. The CIGRE TF 15.01.01 guideline recommends using gas ratios alongside individual gas levels to improve interpretation accuracy. Like the CSUS method, the main drawback of the CIGRE Key Gas approach is that it may indicate several faults at the same time, making precise diagnosis more challenging.

Table II.4 Determination of the type of fault according to the CIGRE method

Key gas	Limit	Fault
C_2H_2	> 20	Arcing
H_2	> 100	Partial discharges
$\sum C_xH_y$	> 1 000	Thermal fault
$\sum CO_x$	> 10 000	Cellulosic degradation

II 4.2 Ratios Methods DGA

II.4.2.1 Dornenburg ratios method:

Proposed in the mid-1970s, the Dornenburg ratio technique represents one of the earliest systematic methods for interpreting dissolved gas analysis data in power transformers [57]. This technique is designed to distinguish among three primary fault mechanisms, namely thermal faults, corona discharges, and arcing phenomena, as presented in Table II.4. For reliable application, the method requires that the concentration of at least one key combustible gas—hydrogen (H_2), methane (CH_4), ethylene (C_2H_4), or acetylene (C_2H_2)—reaches or exceeds twice its corresponding normal limit, as detailed in Table II.5. Furthermore, abnormal conditions may also be inferred when the levels of ethane (C_2H_6) or carbon monoxide (CO) exceed their specified threshold values. [58

Table II.4 Fault classification by Doenburg Ratio Method

Fault	$R_1 = \frac{CH_4}{H_2}$	$R_2 = \frac{C_2H_2}{C_2H_4}$	$R_3 = \frac{C_2H_4}{C_2H_6}$	$R_4 = \frac{C_2H_2}{CH_4}$
Thermal decomposition	**>1.0**	**<0.75**	**<0.3**	**>0.4**
Corona	**<0.1**	/	**<0.3**	**>0.4**
Arcing	**0.1–1.0**	**> 0.75**	**>0.3**	**<0.4**

Table II.5 Permitted limit for Dornenburg Ratio Method

Gas	H_2	CH_4	C_2H_6	C_2H_2	C_2H_4	CO
Limit (ppm)	100	120	65	50	1	350

II.4.2.2 The four ratios method of Rogers:

The Rogers' Four Ratio Method (RFRM) [59] is a widely used diagnostic approach for transformer fault detection based on the analysis of four characteristic dissolved gas ratios: methane to hydrogen (CH_4/H_2), ethane to methane (C_2H_6/CH_4), ethylene to ethane (C_2H_4/C_2H_6), and acetylene to ethylene (C_2H_2/C_2H_4). These ratios are evaluated within predefined ranges, and each range is assigned a specific code from zero to five, as summarized in Table II.6. By combining the resulting codes, the method enables the identification of up to twelve distinct types of transformer faults, which are presented in Table II.7 [60].

Table II.6 Rogers Ratio Code

Gas Ratio	Ranges	Code
$R_1 = \frac{CH_4}{H_2}$	< 0.1	5
	0.1- 1	0
	1—3	1
	> 3	2
$R_2 = \frac{C_2H_2}{C_2H_4}$	< 1	0
	> 1	1
$R_3 = \frac{C_2H_4}{C_2H_6}$	< 1	0
	1-3	1
	> 3	2
$R_4 = \frac{C_2H_6}{CH_4}$	< 0.5	0
	0.5-3	1
	> 3	2

Table II.7 Fault Types as stated in Rogers Ratio Method

No	CH_4/H_2	C_2H_6/CH_4	C_2H_4/C_2H_6	C_2H_2/C_2H_4	Fault type
1	0	0	0	0	No fault
2	1-2	0	0	0	<150 ºC thermal fault
3	1-2	1	0	0	150–200 ºC thermal fault
4	0	1	0	0	200–300 ºC thermal fault
5	0	0	1	0	General conductor overheating
6	1	0	1	0	Winding circulating currents
7	1	0	2	0	Core and tank circulating currents overheated joints
8	5	0	0	0	Partial discharge
9	5	0	0	1-2	Partial discharge with tracking
10	0	0	0	1	Flashover without power follow through
11	0	0	1-2	1-2	Arc with power follow- through
12	0	0	2	2	Continuous sparking to floating potential

II.4.2.3 IEC Ratio Method:

The IEC Ratio Method is widely used for interpreting dissolved gas analysis (DGA) results in power transformers [61]. Although it follows a diagnostic approach similar to the Rogers four-ratio method, it does not include the ethane-to-methane (C_2H_6/CH_4) ratio. Instead, the method relies on standard concentration thresholds for certain key gases, combined with a coding system, to identify potential faults. Three main gas ratios are considered for diagnosis: acetylene to ethylene (C_2H_2/C_2H_4), methane to hydrogen (CH_4/H_2), and ethylene to ethane (C_2H_4/C_2H_6), which are summarized in Table II.8. Detailed fault classifications based on these ratios are presented in Table II.9.

Table II.8 IEC code

Ratio Codes	**Range**	**Code**
R1 = CH_4/H_2	$R1<0.1$	1
	$0.1\leq R1\leq 1$	0
	$R1>1$	2
R2 = C_2H_2/C_2H_4	$R2<0.1$	0
	$0.1\leq R2\leq 3$	1
	$R2>3$	2
R3 = C_2H_4/C_2H_6`	$R3<1$	0
	$1\leq R3\leq 3$	1
	$R3>3$	2

Table II.9 Fault diagnosis using IEC code

N	Fault type	Code		
1	No Fault	0	0	0
2	Partial discharge with low energy density	0	1	0
3	Partial discharge with high energy density	1	1	0
4	discharge of low energy	1.2	0	1.2
5	discharge of high energy	1	0	2
6	Overheating $T<150$ °C	0	1	0
7	Overheating $150<T<300$ °C	2	1	0
8	Overheating $300\leq T\leq 700$ °C	2	1	0
9	Overheating ≥ 700 °C	2	2	2

II.4.2.4 Three-Ratios Technique (TRT)

Gouda et al. developed an advanced diagnostic approach known as the Three-Ratios Technique (TRT) [62], which builds upon previous methods of interpreting insulating gases. This technique relies on three newly defined gas indicators specifically designed to enhance fault detection and provide a more accurate assessment of fault severity. The details and functions of these indicators are presented in Table II.10 [63]

Table II.10 TRT codes

Ratio Codes	Range	Code
$R_1 = \frac{C_2H_2}{C_2H_4}$	R1 < 0.05	0
	0.05 ≤ R1 ≤ 0.9	1
	R1 > 0.9	2
$R_2 = \frac{(C_2H_6 + C_2H_4)}{(H_2 + C_2H_2)}$	R2 < 1	0
	1 ≤ R2 ≤ 3.5	1
	R1 > 3.5	2
$R_3 = \frac{(CH_4 + C_2H_2)}{C_2H_4}$	R3 < 0.05	0
	0.05 ≤ R3 ≤ 0.5	1
	R3 > 0.5	2

II.4.3 Graphical Methods:

Graphical methods are widely used in Dissolved Gas Analysis (DGA) for transformer fault diagnosis. They provide a visual representation of gas data to simplify the identification of different types of electrical and thermal faults.

II.4.3.1 Duval Triangle Method::

The Duval Triangle Method (DTM) is the first alternative graphical method to ratio-based methods for interpreting Dissolved Gas Analysis (DGA). This method was proposed by the Canadian scientist Michel Duval in 1974 [64]. It uses three gas ratios, R1, R2, and R3, which represent a point on a triangular graph as shown in Figure II.1. The triangle is divided into seven fault zones, namely PD, D1, D2, DT, T1, T2, and T3, where the fault is diagnosed according to the region in which the point is located [65]. Michel Duval later extended this method by introducing additional triangles (Duval Triangles 4–7), including Triangle 4 for low-temperature faults and Triangle 5 for high-temperature faults [66], [67]. The ratios used in this method are defined in equations (II.1)–(II.3).

R1=100*CH4/CH4+C2H4+C2H2 (II1)

R2=100*C2H2/CH4+C2H4+C2H2 (II2)

R3=100*C2H4/CH4+C2H4+C2H2 (II3)

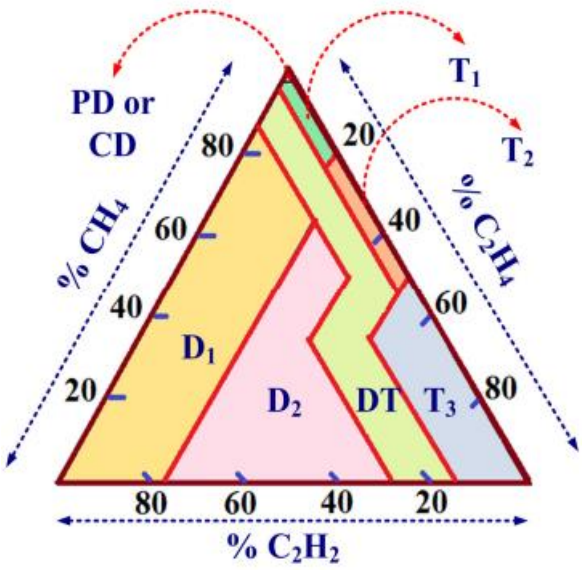

Figure II.4 Duval Triangle 1[64].

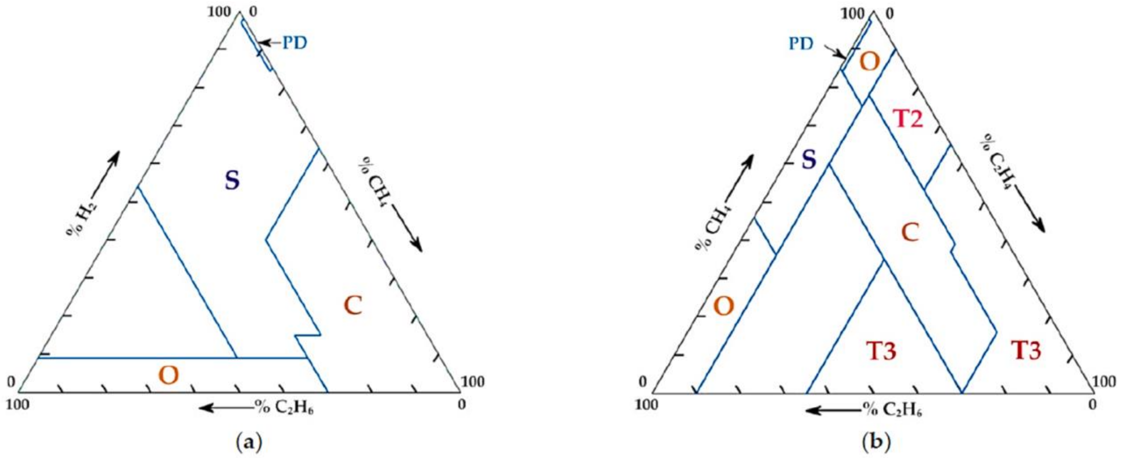

Figure II.5 (a) Duval 4 for a low-temperature fault (b) Duval 5 for a high-temperature fault [66].

II.4.3.2 Duval Pentagon Method:

The Duval Pentagon, developed by Duval and Lamar [68], provides a graphical tool for interpreting DGA results (Figure II.3). It represents the relative concentrations of five key gases—hydrogen (H_2), methane (CH_4), ethane (C_2H_6), ethylene (C_2H_4), and acetylene (C_2H_2)—on a pentagonal chart. The chart is divided into six zones corresponding to thermal and electrical faults, with an additional area for stray gases. Calculations determine the pentagon's position, allowing for accurate and efficient fault diagnosis based on the DGA data.

$$\begin{cases} x_0 = \%H_2\cos(\frac{\pi}{2}) \\ x_1 = \%C_2H_6\cos(\frac{\pi}{2}+\frac{2\pi}{5}) \\ x_2 = \%CH_4\cos(\frac{\pi}{2}+\frac{4\pi}{5}) \\ x_3 = \%C_2H_4\cos(\frac{\pi}{2}+\frac{6\pi}{5}) \\ x_4 = \%C_2H_2\cos(\frac{\pi}{2}+\frac{8\pi}{5}) \end{cases} \begin{cases} y_0 = \%H_2\sin\left(\frac{\pi}{2}\right) \\ y_1 = \%C_2H_6\sin\left(\frac{\pi}{2}+\frac{2\pi}{5}\right) \\ y_2 = \%CH_4\sin\left(\frac{\pi}{2}+\frac{4\pi}{5}\right) \\ y_3 = \%C_2H_4\sin\left(\frac{\pi}{2}+\frac{6\pi}{5}\right) \\ y_4 = \%C_2H_2\sin\left(\frac{\pi}{2}+\frac{8\pi}{5}\right) \end{cases} \qquad \text{(II.4)}$$

$$\mathrm{A} = \frac{1}{2}\sum_{i=0}^{4}(x_i y_{i+1} - x_{i+1} y_i) \qquad \text{(II.5)}$$

$$\begin{cases} X_C = \dfrac{\sum_{i=0}^{4}(x_i + x_{i+1})(x_i y_{i+1} - x_{i+1} y_i)}{6A} \\ Y_C = \dfrac{\sum_{i=0}^{4}(y_i + y_{i+1})(x_i y_{i+1} - x_{i+1} y_i)}{6A} \end{cases} \qquad \text{(II.6)}$$

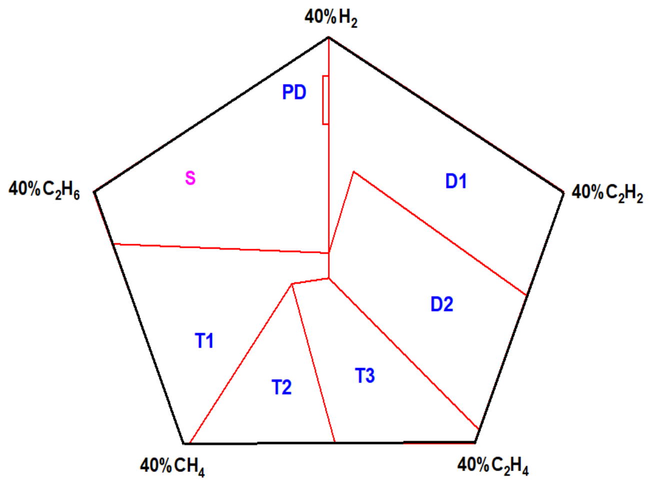

Figure II.6 Duval Pentagon Method [68].

II.4.3.3 Mansour Pentagon Method:

In 2012, Mansour introduced a graphical fault diagnosis method using a pentagon shape [69]. This method was further refined in later studies [70]. It works by plotting the percentage of each specific gas at the vertices of a pentagon, relative to the total gas content. Similar to the Duval Pentagon, the Mansour Pentagon divides the pentagon into six zones, each representing a different type of electrical or thermal fault. The main distinction lies in the fault classification system used, as illustrated in Figure II.4.

The approach relies on a set of equations that relate gas concentrations to their positions on the pentagon, enabling a precise identification of faults and providing engineers with a clear diagnostic tool.

$$s = \sum_{i=1}^{5} P_i \tag{II.7}$$

$$P_{\%i} = \frac{P_i}{s} * 100 \tag{II.8}$$

$$\begin{cases} x_m = \dfrac{\sum_{i=1}^{n} P_{\%i} x_i}{P_{\%i}} \\ y_m = \dfrac{\sum_{i=1}^{n} P_{\%i} y_i}{P_{\%i}} \end{cases} \tag{II.9}$$

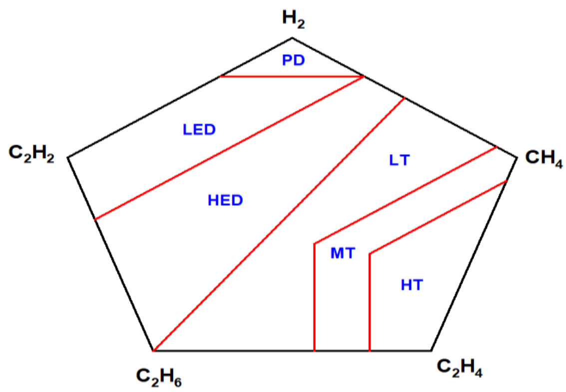

Figure II.7 Mansour Pentagon Method [70].

II.4.3.4 Gouda Triangle Method:

The Gouda Triangle Method (GTM) is an advanced graphical diagnostic technique introduced by Gouda and colleagues [71]. It was designed to improve upon the Duval Triangle Method, which relies solely on three gases for fault detection. GTM enhances fault analysis by adding two more gases, ethane (C2H6) and hydrogen (H2), to the evaluation.

In this method, three ratios, R1, R2, and R3, are first calculated and then converted into percentages P1, P2, and P3, each corresponding to a vertex of a triangle that ultimately forms a parallelogram structure. Like the Duval method, GTM uses a triangular graph to define fault zones, as shown in Figure II.5. The inclusion of the additional gases provides a more detailed and accurate diagnosis of transformer faults, making the method more effective for identifying different types of issues.

$$\begin{cases} R_1 = \dfrac{CH_4}{CH_4 + C_2H_4 + C_2H_6 + C_2H_2} \\ R_2 = \dfrac{C_2H_2}{H_2 + C_2H_6 + CH_4 + C_2H_2} \\ R_3 = \dfrac{C_2H_4}{H_2 + C_2H_6 + CH_4 + C_2H_2} \end{cases} \tag{II.10}$$

$$\begin{cases} P_1 = \dfrac{R_1 \times 100}{R_3 + R_2 + R_1} \\ P_2 = \dfrac{R_2 \times 100}{R_3 + R_2 + R_1} \\ P_3 = \dfrac{R_1 \times 100}{R_3 + R_2 + R_1} \end{cases} \tag{II.11}$$

With

$$\begin{cases} x = 100 - P2 - P3\cos\left(\dfrac{\pi}{6}\right)\cot\left(\dfrac{\pi}{3}\right) \\ y = P3\cos\left(\dfrac{\pi}{6}\right) \end{cases} \tag{II.12}$$

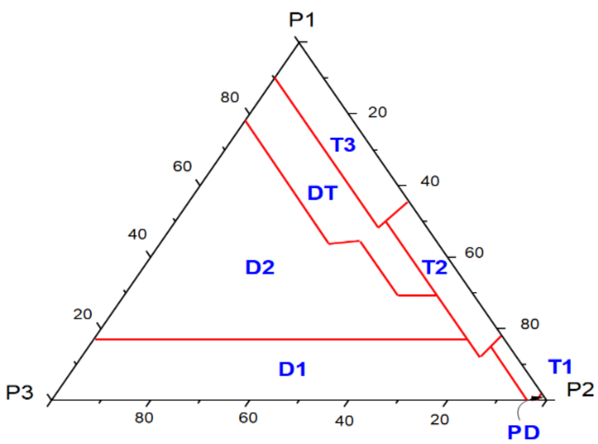

Figure II.8 Gouda Triangle method [71].

II.4.3.5 Gouda heptagon method

The Gouda Heptagon Method, proposed by Gouda et al. in 2018 [72], is a graphical approach for detecting faults in oil-immersed power transformers. It uses a heptagonal chart where each side corresponds to the proportion of one of seven key gases: hydrogen (H_2), methane (CH_4), ethylene (C_2H_4), ethane (C_2H_6), acetylene (C_2H_2), carbon monoxide (CO), and carbon dioxide (CO_2). The gas values are adjusted using specific weighting factors listed in Table II.06 [72]. This method enables the assessment of three levels of cellulose degradation—high (HCCD), medium (MCCD), and low (LCCD) alongside the six primary IEC fault types and combined electrical-thermal faults. Figure III.6 illustrates how the method identifies both degradation levels and fault categories, providing a thorough framework for transformer condition analysis.

Table II.11 Main gas weighting factors in Gouda Heptagon Method

Key gas	H_2	C_2H_4	C_2H_6	CH_4	CO_2	CO	C_2H_2
Weighting factor	3.5	7	5.3846	2.9167	0.14	1	116.6667

$$\mathbf{H_2} = \frac{\mathbf{H_2 \times 3.5 \times 100}}{\mathbf{(3.5 \times H_2) + (2.9167 \times CH_4) + (5.3846 \times C_2H_6) + (7 \times C_2H_4) + (116.6667 \times C_2H_2) + CO + (0.14 \times CO_2)}} \quad \text{(II.13)}$$

$$\mathbf{CH_4} = \frac{\mathbf{CH_4 \times 2.9167 \times 100}}{\mathbf{(3.5 \times H_2) + (2.9167 \times CH_4) + (5.3846 \times C_2H_6) + (7 \times C_2H_4) + (116.6667 \times C_2H_2) + CO + (0.14 \times CO_2)}} \quad \text{(II.14)}$$

$$\mathbf{C_2H_6} = \frac{\mathbf{C_2H_6 \times 5.3846 \times 100}}{\mathbf{(3.5 \times H_2) + (2.9167 \times CH_4) + (5.3846 \times C_2H_6) + (7 \times C_2H_4) + (116.6667 \times C_2H_2) + CO + (0.14 \times CO_2)}} \quad \text{(II.15)}$$

$$\mathbf{C_2H_4} = \frac{\mathbf{C_2H_4 \times 7 \times 100}}{\mathbf{(3.5 \times H_2) + (2.9167 \times CH_4) + (5.3846 \times C_2H_6) + (7 \times C_2H_4) + (116.6667 \times C_2H_2) + CO + (0.14 \times CO_2)}} \quad \text{(II.16)}$$

$$\mathbf{C_2H_2} = \frac{\mathbf{C_2H_2 \times 116.6667 \times 100}}{\mathbf{(3.5 \times H_2) + (2.9167 \times CH_4) + (5.3846 \times C_2H_6) + (7 \times C_2H_4) + (116.6667 \times C_2H_2) + CO + (0.14 \times CO_2)}} \quad \text{(II.17)}$$

$$\mathbf{CO_2} = \frac{\mathbf{CO_2 \times 0.14 \times 100}}{\mathbf{(3.5 \times H_2) + (2.9167 \times CH_4) + (5.3846 \times C_2H_6) + (7 \times C_2H_4) + (116.6667 \times C_2H_2) + CO + (0.14 \times CO_2)}} \quad \text{(II.18)}$$

$$\mathbf{CO} = \frac{\mathbf{CO \times 100}}{\mathbf{(3.5 \times H_2) + (2.9167 \times CH_4) + (5.3846 \times C_2H_6) + (7 \times C_2H_4) + (116.6667 \times C_2H_2) + CO + (0.14 \times CO_2)}} \quad \text{(II.19)}$$

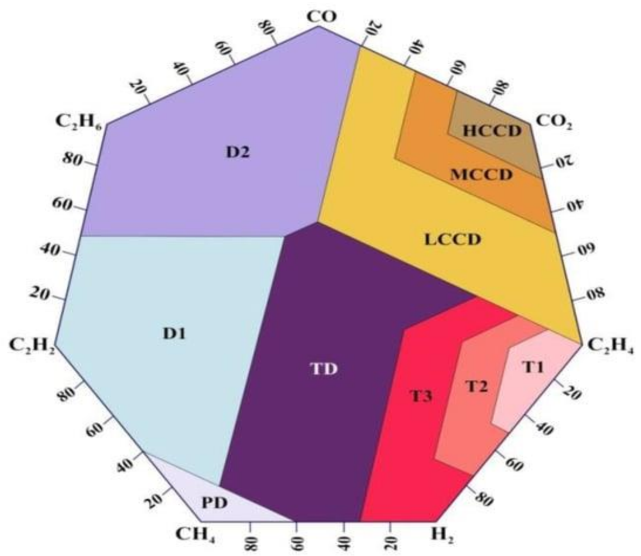

Figure II 9 Gouda’s heptagon Method [72],

II .4.3.6 Cartesian graphical method:

The Cartesian Graphical Method [73], proposed by Fathallah et al., represents one of the most recent advancements in dissolved gas analysis (DGA) and is regarded as a state-of-the-art technique for power transformer fault diagnosis. This method is based on the concentrations of four key gases: hydrogen (H_2), methane (CH_4), ethylene (C_2H_4), and acetylene (C_2H_2). The approach relies on the calculation of three specific ratios that incorporate the concentration of hydrogen (H_2), while also taking into account the influence of ethane (C_2H_6), with the aim of improving the accuracy of fault identification.

$$P_1 = \frac{\mathrm{CH_4} + \mathrm{H_2}}{2 \times \mathrm{H_2} + 2 \times \mathrm{CH_4} + \mathrm{C_2H_2} + \mathrm{C_2H_4}} \qquad \text{(II.21)}$$

$$P_2 = \frac{\mathrm{C_2H_2} + \mathrm{H_2}}{2 \times \mathrm{H_2} + 2 \times \mathrm{CH_4} + \mathrm{C_2H_2} + \mathrm{C_2H_4}} \qquad \text{(II.22)}$$

$$P_3 = \frac{\mathrm{C_2H_4} + \mathrm{CH_4}}{2 \times \mathrm{H_2} + 2 \times \mathrm{CH_4} + \mathrm{C_2H_2} + \mathrm{C_2H_4}} \qquad \text{(II.23)}$$

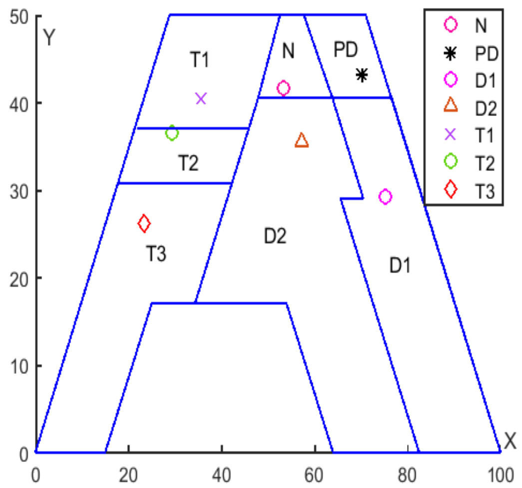

Figure II.10 Cartesian graphical Method [73].

These ratios are subsequently used to determine the Cartesian coordinates (x,y) for graphical representation. The coordinates are computed as follows:

$$x_{\text{point}} = (P_2 + P_1 \times \sin(30°)) \times L \qquad \text{(II.24)}$$

$$y_{\text{point}} = (P_1 \times \sin(60°)) \times L \qquad \text{(II.25)}$$

Where L is a scaling factor.

The obtained coordinates allow the representation of different fault conditions on a Cartesian graph, as illustrated in Figure II.7. This graph is divided into several regions, each corresponding to a specific type of fault, such as partial discharge (PD), low-energy discharge (D1), high-energy discharge (D2), as well as thermal faults at different levels (T1, T2, T3), in addition to the normal operating region (N). This methodology relies on a clear and simple graphical representation, which contributes to improving the accuracy and effectiveness of transformer fault diagnosis.

II.4.3.7 Circle Methods

These methods, proposed by Hechifa et al. [74], apply state-of-the-art graphical techniques in the diagnosis of faults in transformers using DGA. They optimize fault zone separation by dynamically rotating axes to achieve the best spatial distribution of fault samples. Metaheuristic algorithms, such as Gray Wolf Optimization (GWO) and Whale Optimization Algorithm (WOA), are used to determine optimal angles that minimize sample overlap and maximize spacing between fault centers. The methods are mathematically expressed by equations (25) and (26), enhancing the ability to differentiate electrical and thermal faults.

$$x_i = \%H_2\cos(\theta 1) + \%CH_4\cos(\theta 2) - \%C_2H_6\cos(\theta 3) - \%C_2H_4\cos(\theta 4) + \%C_2H_2\cos(\theta 5)$$
(II 26)

$$y_i = \%H_2\sin(\theta 1) + \%CH_4\sin(\theta 2) + \%C_2H_6\sin(\theta 3) - \%C_2H_4\sin(\theta 4) - \%C_2H_2\sin(\theta 5)$$
(II 27)

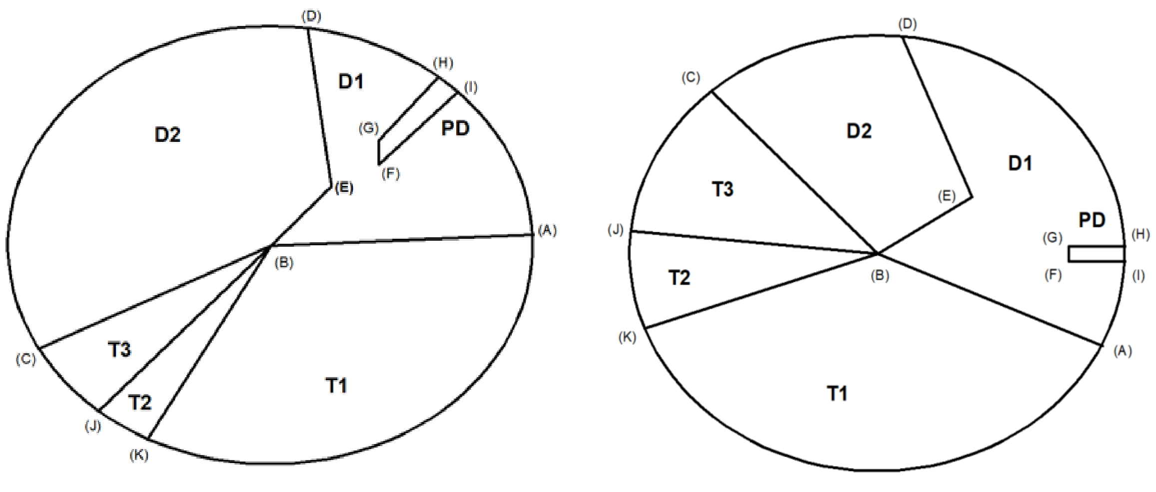

(a) (b)

Figure II.11 final Circle 1(a) and Circle 2(b)

II.5 Conclusion

This chapter presented a comprehensive study of power transformer condition monitoring techniques, with a particular focus on **Dissolved Gas Analysis (DGA)** as one of the most effective and widely used methods for diagnosing internal faults in oil-immersed transformers. The fundamental principles of gas generation within transformers, as well as gas extraction and analysis techniques, were explained. In addition, the evolution of DGA techniques and their critical role in the early detection of electrical and thermal faults, along with the deterioration of oil and paper insulation, were reviewed.

Furthermore, the chapter discussed the most important methods used for interpreting DGA results, including traditional approaches, ratio-based methods, graphical techniques, and advanced diagnostic methods, highlighting the advantages and limitations of each. The study demonstrated that reliance on a single diagnostic method may not always provide an accurate assessment, thereby emphasizing the necessity of combining multiple diagnostic techniques to enhance the reliability and accuracy of fault identification.

In conclusion, this chapter confirms that dissolved gas analysis constitutes a fundamental pillar of condition-based maintenance programs. It plays a vital role in improving the reliability of power transformers, extending their operational lifespan, and reducing the technical and economic risks associated with unexpected failures, thereby contributing to the continuous and efficient operation of electrical power networks.

Chapter III Artificial Intelligence (AI)

III.1 Introduction

The theoretical foundations of machine learning are based on mathematics, particularly statistics, probability theory, linear algebra, and optimization. These foundations enable the development of classification and regression models capable of handling complex and nonlinear data that are difficult to analyze using conventional methods [75].

Machine learning algorithms have demonstrated high effectiveness in diagnostic and classification applications by discovering hidden patterns and relationships within data, thereby improving prediction accuracy and adaptability under varying operating conditions. As a result, machine learning has become a key component of intelligent diagnostic and decision-support systems, reducing reliance on manual analysis and human expertise [76].

Artificial Intelligence (AI) is a major branch of computer science that aims to develop systems capable of performing tasks that normally require human intelligence, such as learning, reasoning, decision-making, and problem-solving. According to the Encyclopaedia Britannica, AI refers to the ability of machines to perform tasks traditionally associated with human intelligence [77].

The field formally emerged during the Dartmouth Conference in 1956, where John McCarthy introduced the term “Artificial Intelligence,” marking the beginning of extensive research in this domain [78]. Since then, AI has evolved from rule-based systems to modern data-driven approaches that rely on large datasets and advanced algorithms, significantly enhancing its ability to solve complex problems [79].

AI relies on data, algorithms, and learning from experience to build intelligent models capable of improving their performance over time. It is an interdisciplinary field that integrates concepts from mathematics, statistics, and cognitive sciences [80].

Today, AI is widely applied in healthcare, industry, transportation, security, and natural language processing, making it a fundamental technology in digital transformation. However, its rapid adoption also raises ethical and legal concerns related to privacy, bias, and accountability in automated decision-making systems [81].

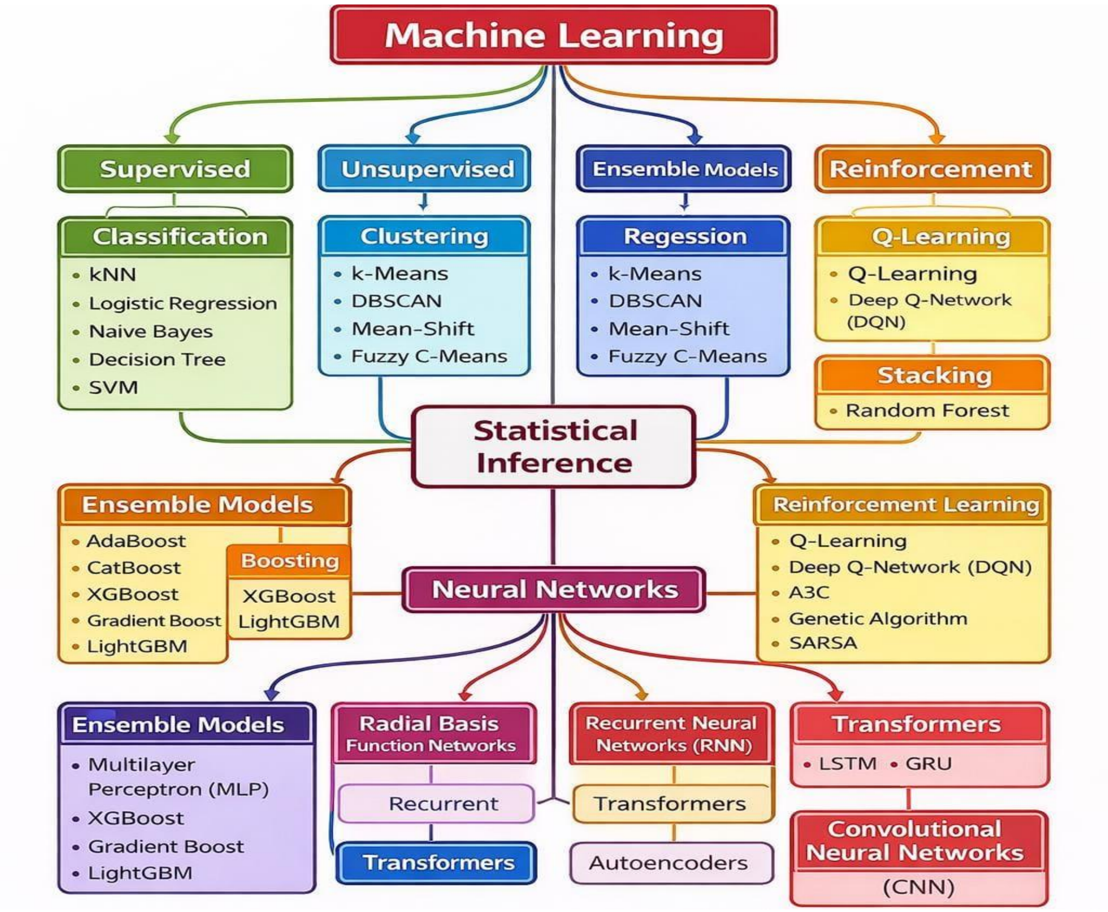

Figure III.1 General Classification of Machine Learning Algorithms and Their Core Models [82].

Through this diagram, we will address the concepts of Machine Learning and Neural Networks. We will also focus on explaining the following algorithms: SVM, AdaBoost Random Forest, and KNN.

III.2 Foundations of Machine Learning (ML)

Machine Learning (ML) is a subfield of artificial intelligence that focuses on developing computational methods that allow systems to automatically improve their performance on a task through experience. Unlike traditional programming, where explicit rules are coded for every scenario, ML systems learn patterns and relationships from data to make predictions, classifications, or decisions[83].

The foundation of ML combines mathematical modeling, statistical analysis, optimization theory, and computer science techniques to construct models that can generalize from observed data to unseen scenarios. This ability to generalize is central to ML and distinguishes it from memorization or simple rule-based systems[84].

Machine learning tasks are commonly formulated as constrained or unconstrained minimization problems. The learning process involves optimizing a loss function that quantifies the discrepancy between predicted and actual outputs. Regularization techniques are often incorporated to penalize overly complex models and improve generalization, particularly when dealing with noisy or limited datasets [85].

The theoretical foundations of machine learning provide the essential mathematical and algorithmic framework for constructing intelligent models capable of learning from data. These foundations enable machine learning methods to operate effectively in high-dimensional and nonlinear problem domains, making them well suited for advanced diagnostic and decision-support applications [86].

III.2.1 Types of Machine Learning

Machine learning algorithms can be categorized into several learning paradigms according to the availability of labeled data and the way knowledge is acquired from the training process. The three main types are supervised learning, unsupervised learning, and reinforcement learning. Each paradigm follows a different learning strategy and is suitable for specific applications depending on the nature of the problem and the characteristics of the available data.

III.2.2.1 Supervised Learning Concept

Supervised Learning is a central paradigm in machine learning in which a model is trained using labeled data to learn the underlying relationship between input features and corresponding output labels. In this framework, the learning algorithm is “supervised” by the provided labels, meaning it receives direct feedback on its predictions during training. This enables the model to generalize from the observed examples and make accurate predictions for new, unseen data [87].

The supervised learning paradigm provides a robust theoretical foundation for developing intelligent diagnostic systems. Its reliance on labeled data allows models to achieve high predictive accuracy and interpretability, making supervised learning particularly suitable for classification-based decision support and fault diagnosis tasks in complex engineering systems [88].

III.2.2.2 Unsupervised Learning

Unsupervised Learning is a key paradigm in machine learning where the algorithm is trained on unlabeled data, meaning that the output labels yi are unknown. Instead of being guided by correct answers, the algorithm explores the structure and patterns within the input data xi to identify relationships, groupings, or underlying distributions[89].

In contrast to supervised learning, unsupervised learning focuses on discovering hidden patterns, clusters, or representations in the data, rather than predicting specific outputs.

Learning methods are widely used across various fields, including customer behavior analysis, image and text processing, fraud detection, and organizing large datasets. These methods are particularly useful when labeled data are unavailable or difficult to obtain, making them a powerful tool for exploratory data analysis and understanding the internal structures of complex systems [90].

III.2.2.3 Reinforcement Learning

Branch of machine learning that focuses on sequential decision-making through the interaction of a model, known as an agent, with its surrounding environment. In this type of learning, the agent is not provided with predefined correct outputs for each state. Instead, it learns through trial and error by receiving rewards or penalties based on the actions it takes. The agent's primary objective is to maximize the cumulative long-term reward, that is, to learn an optimal policy that achieves the best possible outcomes [91].

Reinforcement Learning (RL) is a fundamental paradigm of machine learning in which an agent learns to make decisions by interacting with an environment. Unlike supervised learning, RL does not rely on labeled input-output pairs; instead, the agent learns through trial and error by receiving feedback in the form of rewards or penalties. The objective of the agent is to learn a policy that maximizes the cumulative reward over time [92].

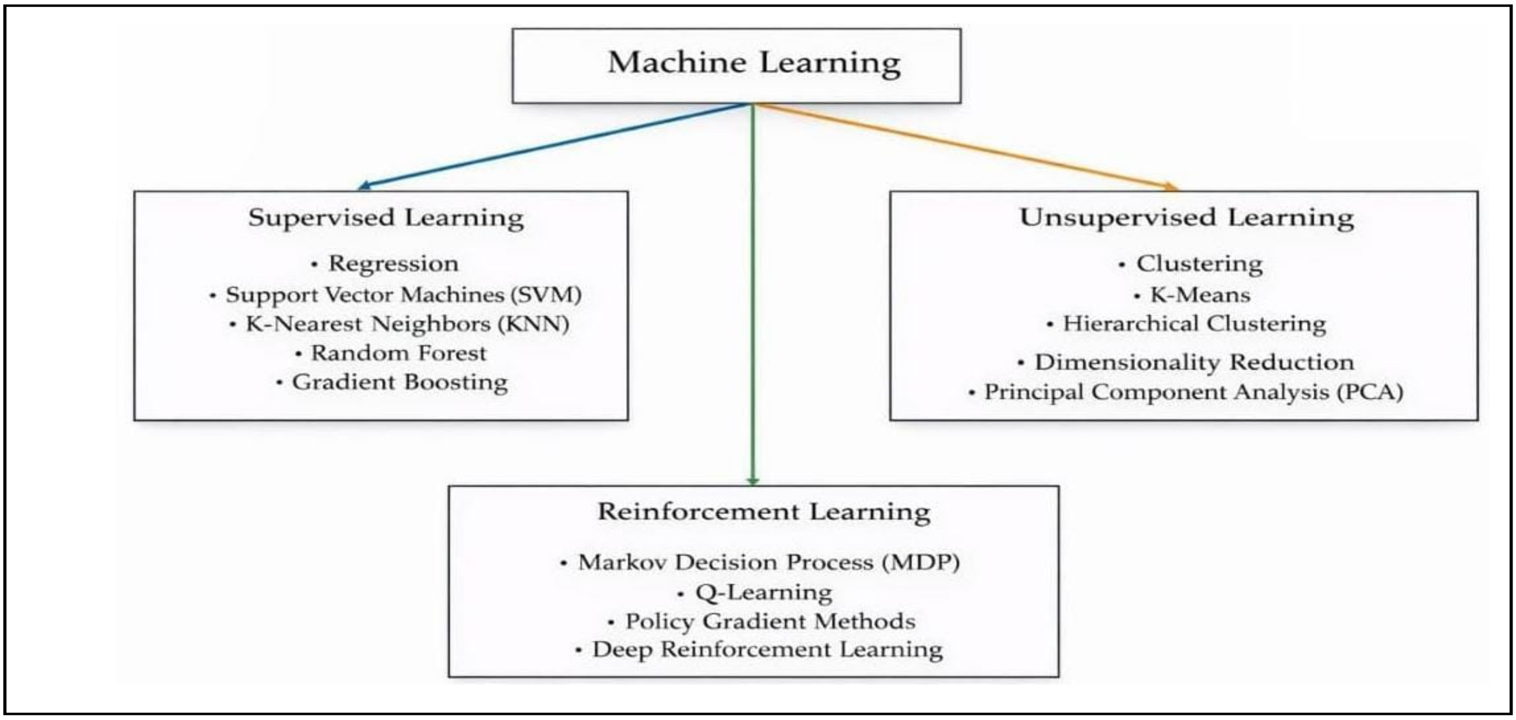

Figure III.2 Taxonomy and Paradigms of Machine Learning Methods [93].

III.3 Deep Learning

Deep Learning (DL) is a subfield of machine learning that focuses on learning data representations through artificial neural networks (ANNs) with multiple layers. Unlike traditional machine learning models, which often rely on manually engineered features, deep learning models can automatically extract hierarchical features from raw data, enabling them to handle complex, high-dimensional data such as images, audio, and natural language [94].

III.4 Ensemble Learning

Ensemble Learning is a machine learning approach that consists of combining multiple base learners to produce a final model that is more accurate and stable. This approach is based on the principle that aggregating several models helps reduce bias and variance errors, thereby improving the model's generalization ability [95].

This framework is built upon three main components

III.4.1 Base Learners:

These can be homogeneous models (e.g., multiple decision trees) or heterogeneous models (e.g., combining SVM, KNN, and decision trees).

III.4.2 Diversity Mechanism:

Ensures variation among models through techniques such as bootstrap sampling, hyperparameter tuning, or using different algorithms.

III.4.3 Aggregation Strategy:

Combines model outputs using methods such as majority voting for classification, averaging for regression, or a meta-learner in the case of stacking.

Ensemble Learning techniques are generally categorized into three main strategies:

Bagging: e.g., Random Forest, which reduces variance by training models on different data samples.

Boosting: e.g., AdaBoost, where models are trained sequentially, each focusing on correcting the errors of previous ones [96].

III.5 Study of Proposed Classification Algorithms

This section introduces the machine learning algorithms used for classification in this study, namely SVM, k-NN, Decision Trees, and AdaBoost. These methods are widely applied in pattern recognition and fault diagnosis due to their efficiency in handling complex datasets and their different learning strategies.

III 5.1 Support Vector Machine (SVM)

(SVM) represent one of the advanced classification methods in machine learning and were developed based on Vapnik's research in the 1990s. This algorithm relies on a discriminant function to determine the optimal hyperplane that effectively separates different classes within a dataset. SVM is recognized for its high accuracy and robustness in classification, whether dealing with linear or nonlinear data, making it well-suited for data mining applications and complex analyses [97]. Figure III.3 illustrates the general structure of the SVM algorithm, which works by identifying the optimal separating hyperplane, mathematically defined by the following equation:

$$f(x)=w\mathrm{T}\ x+b \qquad \text{for all } i \qquad \text{(III.1)}$$

Where w is the weight vector, x is the input feature vector, and b is the bias. The objective is to maximize the margin 2‖w‖ between the classes, subject to the constraints w is the weight vector, x is the input feature vector, and b is the bias. The objective is to maximize the margin $\frac{2}{\|w\|}$ between the classes, subject to the constraints:

$$w\ \mathrm{T}x\mathrm{i}+\ b)\geq 1 \qquad \text{(III.2)}$$

yi the effectiveness of Support Vector Machines (SVM) largely depends on the selection of the Kernel Function, which enables the transformation of the input space into a higher-dimensional feature space. This transformation allows the model to perform linear discrimination efficiently, even when dealing with complex or nonlinear data [98].

Kernel Trick can be represented as

$$K\ (xi,\ xj)=\phi(xi)\mathrm{T}\ \phi(xj) \qquad \text{(III.3)}$$

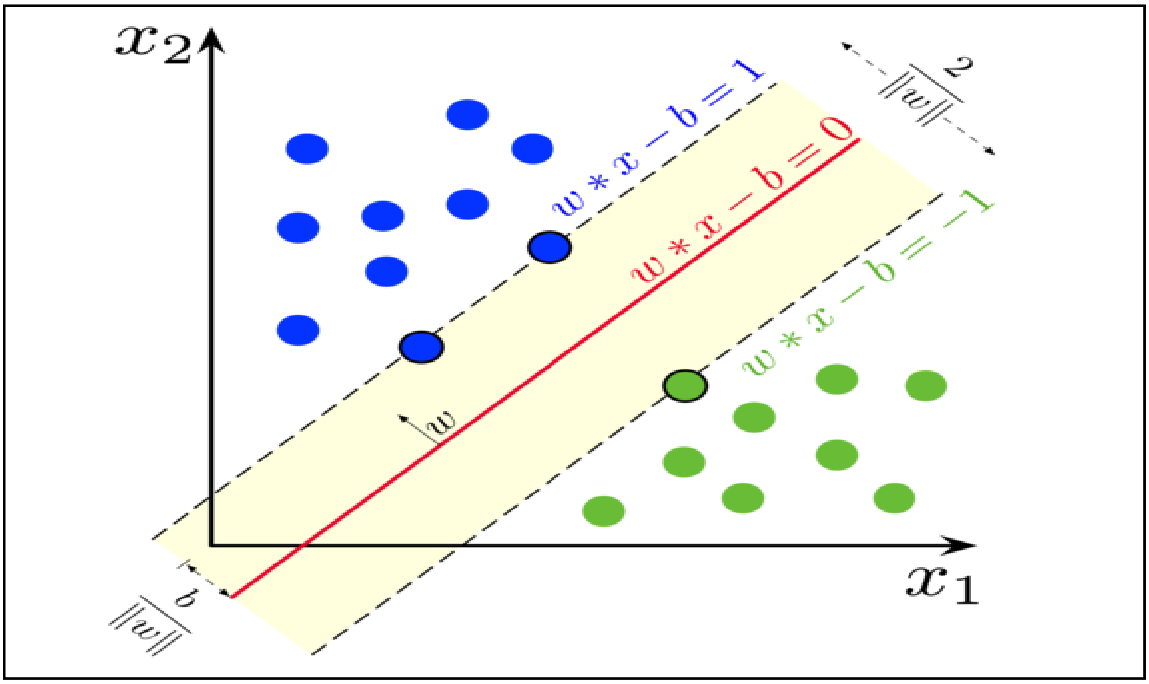

Figure III.3 Enhanced Hyperplane Optimization in SVM for High-Dimensional Data Classification[98].

III 5.2 k-Nearest Neighbors (k-NN)

The K-Nearest Neighbor (KNN) algorithm is considered one of the simplest learning algorithms, as it does not rely on a traditional training phase. Instead, it stores the training data and uses it directly during the classification process. Its mechanism is based on calculating the distance between a query point and the data points in the dataset, then selecting the closest k points. The class label assigned to the new point is determined by the class that appears most frequently among these nearest neighbors [99].

This can be mathematically expressed as:

$$\hat{y} = \operatorname{argmax}_c \sum_{j=1}^{k} I(y_j = c) \qquad \text{(III. 4)}$$

where I is an indicator function that equals 1 if the class label yj matches c and 0 otherwise. The distance between points is often measured using Euclidean distance:

$$d(x_i, x_j) = \sqrt{\sum_{k=1}^{n} (x_{ik} - x_{jk})^2} \qquad \text{(III.5)}$$

This method enhances the classification process by extending the nearest neighbor concept, allowing the algorithm to leverage more information from multiple nearby points during the d

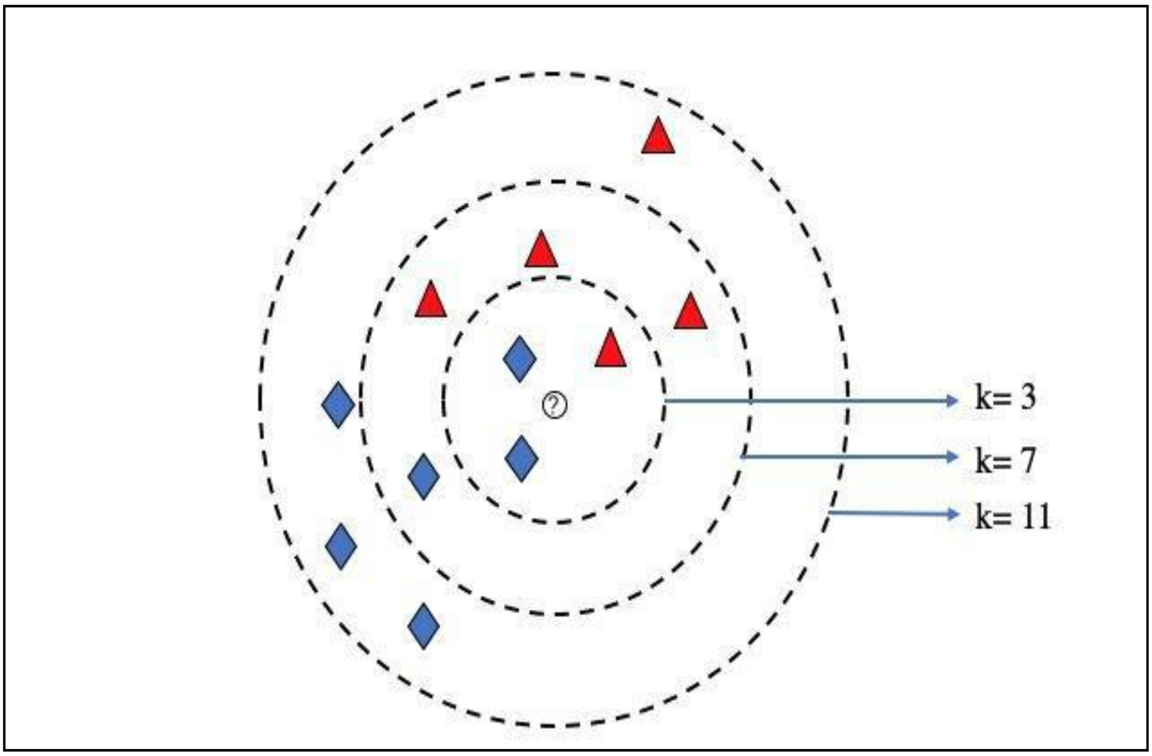

Figure III .4 Principle of KNN algorithm with different k value[100].

III.5.3 Decision Trees (DT)

Decision Trees (DT) are a widely recognized classification algorithm known for their relatively simple structure. They excel at accurately analyzing substantial amounts of data within a short timeframe, making them particularly well-suited for efficient mass data processing [101]. The DT classifier is constructed using a combination of internal nodes and leaf nodes, where internal nodes represent decision thresholds based on feature values, and leaf nodes correspond to the predicted class labels as in Figure III.5. The training process involves recursively identifying the best partition at each node to minimize uncertainty about the class labels, commonly assessed through metrics such as Entropy and Gini Impurity [102].

Entropy is calculated as:

$$H(S) = -\sum_{i=1}^{c} p_i \log_2 p_i \qquad \text{(III.6)}$$

Gini Index is defined as:

$$IG(S,A) = H(S) - \sum_{v \in A} \frac{|S_v|}{|S|} H(S_v) \tag{III.7}$$

where p_i is the probability of class i in set S.

Information Gain is used to determine the best feature to split on:

$$\text{Gini}(S) = 1 - \sum_{i=1}^{c} (p_i)^2 \tag{III.8}$$

This process continues until the dataset is fully analyzed, ensuring that each path through the tree leads to a definitive classification outcome.

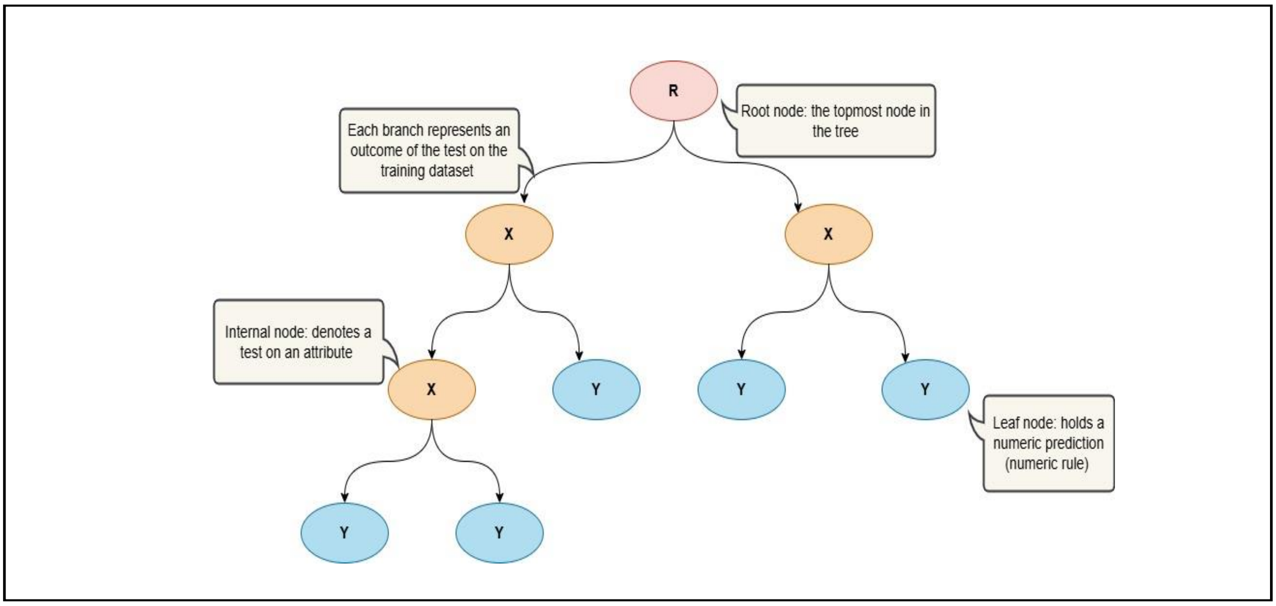

Figure III.5 Decision tree structure[103].

III 5.4 AdaBoost

The AdaBoost algorithm, short for Adaptive Boosting, is a supervised machine learning technique that combines several weak learners, usually shallow decision trees (decision stumps), to build a strong classifier. AdaBoost works by training models sequentially, where each new model focuses more on the samples that were misclassified by previous models.

AdaBoost assigns weights to training samples. Initially, all samples have equal weights, but after each iteration, the weights of incorrectly classified samples are increased so that the next weak learner pays more attention to them. The final prediction is obtained through a weighted vote of all weak learners.

AdaBoost is widely used because of its simplicity, high classification performance, and ability to improve weak classifiers. However, it can be sensitive to noisy data and outliers since difficult samples receive higher importance during training[103].

III 5.4.1 AdaBoost Model (Ensemble of Weak Learners)

In AdaBoost, the final model is represented as a weighted sum of weak classifiers:

$$\hat{y}_i = \text{sign}\left(\sum_{t=1}^{T} \alpha_t h_t(x_i)\right) \qquad \text{(III.9)}$$

where:

$\hat{y}_i$ .Final predicted class for sample i,

T .Total number of weak learners,

$h_t(x_i)$ Prediction of weak learner t for sample x_i,

α_t . Weight assigned to weak learner t,

x_i . Feature vector of sample i,

III 5.4.2 Weak Learner Weight Calculation

The importance of each weak learner is computed according to its classification error:

$$\alpha_t = \frac{1}{2}\ln\left(\frac{1-\varepsilon_t}{\varepsilon_t}\right) \qquad \text{(III.10)}$$

where:

α_t : Weight of weak learner t,

ε_t : Classification error of weak learner t,

$\ln(\cdot)$: Natural logarithm function.

A lower classification error produces a larger α_t, meaning the weak learner has a stronger influence on the final prediction.

III 5.4.3 Sample Weight Update

After each iteration, sample weights are updated to emphasize misclassified samples:

$$w_i^{(t+1)} = w_i^{(t)} \exp\left(-\alpha_t y_i h_t(x_i)\right) \qquad \text{(III.11)}$$

Then the weights are normalized:

$$w_i^{(t+1)} = \frac{w_i^{(t+1)}}{\sum_{j=1}^{N} w_j^{(t+1)}} \qquad \text{(III.12)}$$

where:

$w_i^{(t)}$: Weight of sample i at iteration t,

y_i : True class label of sample i,

$h_t(x_i)$: Prediction of weak learner t,

N : Total number of samples.

Misclassified samples receive larger weights, allowing the next weak learner to focus more on difficult cases.

III 5.4.4 AdaBoost Multi-Class Classification

For multi-class problems, AdaBoost can be extended using the SAMME algorithm, where the final class prediction is determined by:

$$\hat{y}_i = \arg\max_{k \in \{1,\ldots,K\}} \sum_{t=1}^{T} \alpha_t I(h_t(x_i) = k) \qquad \text{(III.13)}$$

where:

K : Number of classes,

$I(\cdot)$: Indicator function that equals 1 if the prediction belongs to class k, otherwise 0.

α_t : Weight of weak learner t,

$h_t(x_i)$: Predicted class by learner t,

arg max: Selects the class with the highest accumulated score.

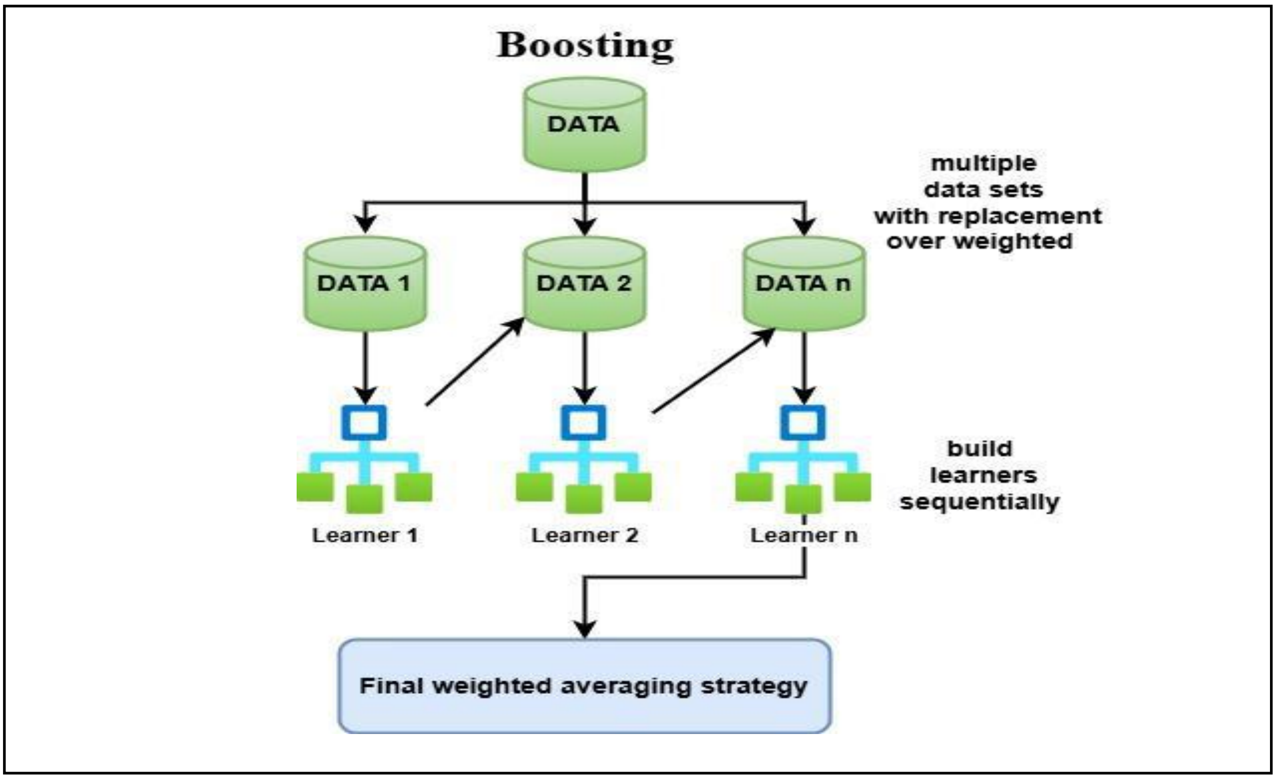

Figure III.6 Structure of Boosting[104].

III. 6 Performance evaluation metrics in classification

Are used to assess a model's ability to correctly classify samples into their respective categories. These metrics help compare different models, identify their strengths and weaknesses, and improve model performance before practical deployment.

III. 6.1. Confusion Matrix

The confusion matrix is a fundamental tool for summarizing classification performance, consisting of four elements in the case of binary classification:

	Predicted Positive	**Predicted Negative**
Actual Positive	True Positive (TP)	False Negative (FN)
Actual Negative	False Positive (FP)	True Negative (TN)

- **TP (True Positive):** Number of positive samples correctly classified.
- **TN (True Negative):** Number of negative samples correctly classified.
- **FP (False Positive):** Number of negative samples incorrectly classified as positive.
- **FN (False Negative):** Number of positive samples incorrectly classified as negative.

III .6.2 Accuracy

Represents the proportion of correctly classified samples out of the total samples:

$$\text{Accuracy} = \frac{TP}{TP+TN+FP+FN} \qquad \text{(III.14)}$$

Where:

TP (True Positives): Positive samples correctly predicted as positive

TN (True Negatives): Negative samples correctly predicted as negative

FP (False Positives): Negative samples incorrectly predicted as positive

FN (False Negatives): Positive samples incorrectly predicted as negative

Interpretation:

High accuracy → Most predictions (both positive and negative) are correct.

Low accuracy → Many predictions are wrong.

Suitable for balanced datasets, but may be misleading in the case of imbalanced classes.

III.6.3. Precision and Recall

Precision: The proportion of correctly predicted positive samples out of all samples classified as positive by the model:

$$\text{Precision} = \frac{TP}{TP+TF} \qquad \text{(III.15)}$$

TP (True Positives): Correctly predicted positives

FP (False Positives): Incorrectly predicted positives

Interpretation:

High precision → Most of the predicted positives are correct.

Low precision → Many predicted positives are actually negative (false alarms)

Recall (Sensitivity): The proportion of positive samples correctly classified out of all actual positive samples:

$$\text{Recall} = \frac{TP}{TP+FN} \qquad \text{(III.16)}$$

TP (True Positives): Correctly predicted positives

FN (False Negatives): Positives that the model missed

Interpretation:

High recall → The model catches most of the actual positives.

Low recall → The model misses many positives.

III 6.4 F1-Score

The harmonic mean of precision and recall, particularly useful when dealing with imbalanced classes:

$$F1 = 2 \cdot \frac{\text{Precision.Recal}}{\text{Precision} + \text{Recal}} \qquad \text{(III.17)}$$

III 6.5 ROC Curve and AUC

Plots True Positive Rate (TPR / Recall) vs False Positive Rate (FPR) at various thresholds.

Shows the model's performance across all possible thresholds, not just a fixed one.

Formulas:

$$TPR = \frac{TP}{TP+FN} \qquad \text{(Recall)} \qquad \text{(III.18)}$$

$$FPR = \frac{FP}{FP+TN} \qquad \text{(III.19)}$$

TPR = fraction of actual positives correctly detected

FPR = fraction of actual negatives incorrectly classified as positive

AUC (Area Under the Curve): Represents the model's ability to discriminate between classes. The closer the AUC is to 1, the better the model performance.

Important Notes on Metric Selection

Balanced datasets: Accuracy is usually sufficient.

Imbalanced datasets: F1-Score or AUC is preferred.

High cost of false negatives (e.g., disease detection): Focus on **Recall.**

High cost of false positives (e.g., spam detection): Focus on **Precision.**

III .7 CONCLUSION

This chapter established the theoretical and mathematical foundations underlying Artificial Intelligence (AI) and Machine Learning (ML), with a particular emphasis on classification methodologies for intelligent decision-support systems. The evolution from symbolic AI to data-driven learning models reflects a paradigm shift toward optimization-based and statistically grounded computational intelligence.

Machine Learning was formulated within the framework of empirical risk minimization, where predictive functions are learned from data through loss optimization under regularization constraints to ensure generalization. This balance between model complexity and predictive accuracy constitutes the core principle governing modern classification algorithms, especially in high-dimensional and nonlinear environments.

The principal learning paradigms were examined, with supervised learning identified as the most relevant framework for discriminative classification tasks. Its reliance on labeled data enables explicit decision boundary construction and measurable performance evaluation. Unsupervised and reinforcement learning were positioned within broader contexts of structural inference and sequential decision optimization, respectively.

Advanced modeling strategies were analyzed to highlight their contribution to predictive robustness. Deep Learning was characterized as a hierarchical nonlinear function approximation framework capable of learning complex feature representations. Ensemble Learning was interpreted through the bias–variance tradeoff perspective, where aggregation mechanisms improve generalization and reduce overfitting.

The selected algorithms—Support Vector Machine (SVM), K-Nearest Neighbors (KNN), Decision Tree (DT), and AdaBoost —were analytically positioned according to their structural and optimization properties. SVM was presented as a convex margin-maximization classifier with kernel-based nonlinear extension. KNN was described as a non-parametric, distance-based local decision model. Decision Tree was framed as a hierarchical, rule-based model that recursively partitions the feature space to form interpretable decision boundaries. AdaBoost was analyzed as a regularized gradient boosting framework performing sequential functional optimization for enhanced accuracy and convergence stability.

Finally, a multidimensional evaluation framework was introduced, incorporating Accuracy, Precision, Recall, F1-score, and ROC-AUC metrics. The importance of metric selection based on dataset characteristics and risk sensitivity was emphasized to ensure statistically sound comparative analysis.

Overall, this chapter provides a coherent analytical foundation that integrates statistical learning theory, optimization principles, ensemble methodologies, and discriminative evaluation criteria, thereby establishing the theoretical basis for the experimental validation and performance comparison of the proposed classification models.

Chapter IV. Application and Evaluation of AI Technique for Diagnosis

IV.1 Introduction

This chapter provides an in-depth analysis of the results obtained from the application of the proposed methodology for power transformer fault diagnosis, which is grounded in state-of-the-art artificial intelligence techniques. The adopted framework emphasizes enhancing input data quality through dimensionality reduction using the SHAP technique, which offers an interpretable mechanism based on Shapley values. This approach enables a precise quantitative assessment of each feature’s contribution to the model output, thereby improving both model efficiency and interpretability—an essential requirement in intelligent diagnostic systems for critical industrial applications.

Subsequently, a set of advanced classification algorithms was employed, including K-Nearest Neighbors (KNN), Decision Tree (DT), Support Vector Machine (SVM), and the AdaBoost algorithm based on ensemble learning. This diversity of models enabled the development of a comprehensive and reproducible experimental framework aimed at conducting a rigorous comparative evaluation of their performance across multiple criteria, including predictive accuracy, statistical stability, and generalization capability on unseen data. The objective of this evaluation is to identify the most suitable model in terms of the trade-off between predictive performance and interpretability, in alignment with the characteristics of the studied dataset.

The experimental findings demonstrate that the integration of SHAP-based dimensionality reduction with the selected classification algorithms yields significant improvements over conventional and state-of-the-art baseline methods, both in terms of predictive performance and model robustness. Furthermore, this integration enhances the interpretability of model decisions, thereby strengthening the reliability of the proposed system and supporting its applicability in real-world operational environments. Consequently, the proposed framework represents an effective and scalable approach for power transformer fault diagnosis using interpretable artificial intelligence techniques.

IV.2 Experimental setup for AI application for DGA

Researchers and engineers are exploring innovative approaches that focus on achieving precise diagnostics to ensure the safety of power equipment and extend the lifespan of electrical systems, particularly power transformers. In this context, the proposed methodology aims to provide advanced solutions for transformer fault diagnosis, combining high accuracy with interpretability.

The process begins with careful data collection, followed by transforming the data into input vectors suitable for modeling. A normalization step is applied to standardize the data and improve training stability. To address class imbalance, synthetic data is generated, resulting in a balanced dataset that better represents all fault categories.

Both the original and synthetic datasets are then used to evaluate classification algorithms, which are further enhanced using ensemble techniques to improve overall accuracy and robustness. To ensure transparency and interpretability, the SHAP (Shapley Additive Explanations) framework is integrated, allowing the contribution of each input variable—such as dissolved gas concentrations—to be quantified in the final predictions. This integration helps explain model decisions, supports engineering insights, and ensures that the diagnostic process is both accurate and interpretable. The sequential steps of this methodology are visually illustrated in **Figure IV.1**, with detailed explanations provided within this section.

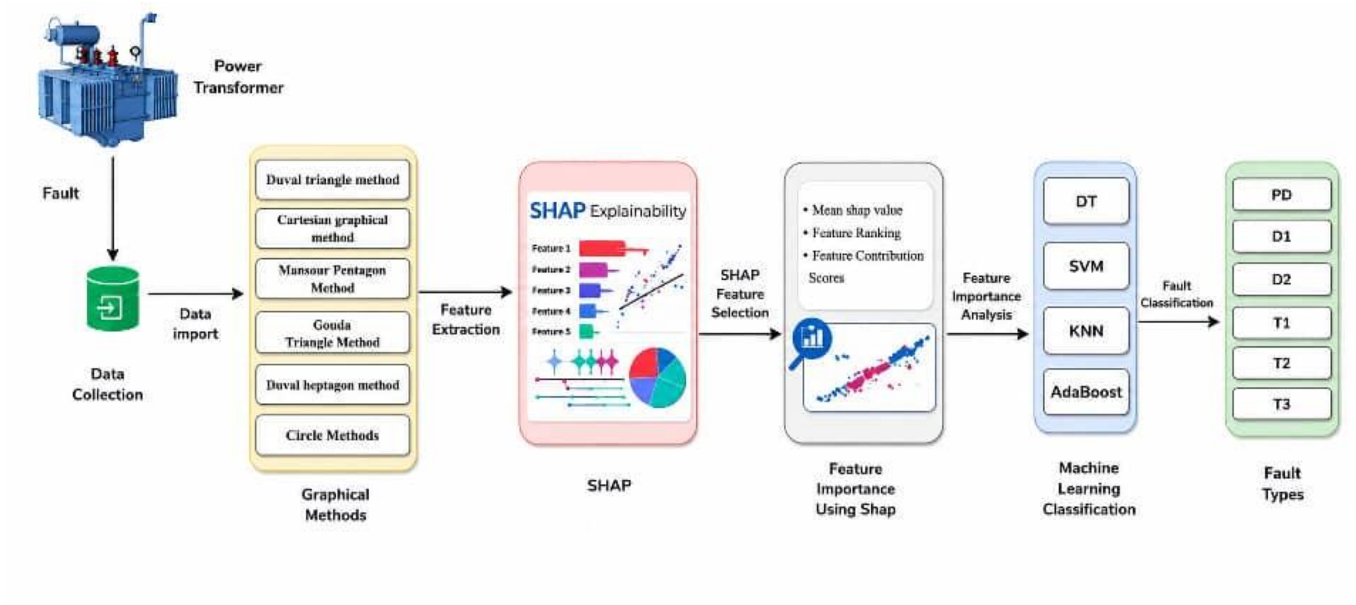

Figure IV.1 Proposed methodology

IV.2. 1 DGA Data Collection

Data collection is an important and crucial step in order to evaluate the condition of power transformers, especially since they suffer from a lack of reliable data sources. 407 samples were collected in this chapter to evaluate the proposed method .

IV.2.2 Input vectors

The process of transforming raw data into input vector features is a critical and fundamental step when employing graphical diagnostic methods to identify transformer faults and analyze the gases generated from oil decomposition. These methods include the Duval Triangle, Duval Pentagon, Mansour Pentagon, and Gouda Triangle, as well as the Cartesian Graphical Method and the Circular Graphical Method. The main purpose of this transformation is to separate overlapping gases and reduce interference between gas signals, ensuring high accuracy in fault analysis and classification. To achieve this, all required features are consolidated into a single unified input vector, which serves as the starting point for each graphical method, allowing precise plotting and classification of faults based on the concentrations and ratios of different gases. Table IV.1 provides a summary of the features composing this vector, including the primary gases and their ratios used across all the aforementioned graphical method.

Table IV.1 Aggregation of features of graphical methods into the proposed input vector

Graphical methods	features equation
Duval Triangle Method	$F1 = x = 100 - \%C_2H_2 - \%CH_4\, cos\left(\frac{\pi}{6}\right) cot\left(\frac{\pi}{3}\right)$ $F2 = y = \%CH_4\, cos\left(\frac{\pi}{6}\right)$
Gouda triangle method	$F3 = x = 100 - \%R_2 - \%R_3\, cos\left(\frac{\pi}{6}\right) cot\left(\frac{\pi}{3}\right)$ $F4 = y = \%R_3\, cos\left(\frac{\pi}{6}\right)$
Duval Pentagon Method	$F5 = X(1) = \frac{1}{6}\frac{\sum_{i=0}^{4}(x_i + x_{i+1})(x_i y_{i+1} - x_{i+1} y_i)}{\frac{1}{2}\sum_{i=0}^{4}(x_i y_{i+1} - x_{i+1} y_i)}$ $F6 = X(2) = \frac{1}{6}\frac{\sum_{i=0}^{4}(y_i + y_{i+1})(x_i y_{i+1} - x_{i+1} y_i)}{\frac{1}{2}\sum_{i=0}^{4}(x_i y_{i+1} - x_{i+1} y_i)}$
Mansour Pentagon Method	$F7 = x_m = \frac{\sum_{i=1}^{n} m_i x_i}{100}$ $F8 = y_m = \frac{\sum_{i=1}^{n} m_i y_i}{100}$
Cartesian graphical method	$F9 = x_{\text{point}} = (P_2 + P_1 \times \sin(30°)) \times L$ $F10 = y_{\text{point}} = (P_1 \times \sin(60°)) \times L$
Circle Methods	$F11 = x_i = \%H_2 \cos(\theta 1) + \%CH_4 \cos(\theta 2) - \%C_2H_6 \cos(\theta 3) - \%C_2H_4 \cos(\theta 4) + \%C_2H_2 \cos(\theta 5)$ $F12 = y_i = \%H_2 \sin(\theta 1) + \%CH_4 \sin(\theta 2) + \%C_2H_6 \sin(\theta 3) - \%C_2H_4 \sin(\theta 4) - \%C_2H_2 \sin(\theta 5)$
Proposed vector	V=[F1, F2, F3, F4, F5, F6, F7, F8, F9, F10, F11, F12]

IV.2.3 SHAP data creation

The SHAP (SHapley Additive exPlanations) method is recognized as one of the most influential and widely adopted approaches for interpreting machine learning models. Introduced in 2017 by Scott M. Lundberg and Su-In Lee at the University of Washington, SHAP is grounded in the concept of Shapley Values derived from Game Theory. The method aims to fairly quantify the contribution of each feature to the final prediction generated by a machine learning model. Owing to its model-agnostic nature, SHAP can be effectively applied to both traditional statistical models, such as linear regression, and more sophisticated machine learning techniques, including random forests and deep neural networks[102].

A major strength of SHAP lies in its ability to provide consistent and theoretically sound explanations of model behavior. The framework evaluates the influence of each feature by comparing the model output across different combinations of input variables and assigning contribution scores accordingly. Mathematically, the prediction explanation can be expressed as follows:

$$f(x) = \phi_0 + \sum_{i=1}^{M} \phi_i \qquad \text{(IV.1)}$$

Where

$\boldsymbol{f(x)}$ denotes the model prediction.

$\boldsymbol{\phi_0}$ represents the baseline or expected model output.

$\boldsymbol{\phi_i}$ corresponds to the SHAP value associated with feature **i**.

reflecting its contribution to the prediction. Through the aggregation of these feature contributions, SHAP produces an interpretable explanation of the model’s decision-making process.

Furthermore, SHAP provides several advanced visualization tools, including bar plots, beeswarm plots, dependence plots, and waterfall plots, which facilitate the interpretation of feature importance and the direction of their impact on predictions. Consequently, SHAP has become an essential technique for enhancing transparency, interpretability, and trustworthiness in artificial intelligence systems. In addition, it supports feature selection, assists in identifying the most influential variables, and promotes the development of more reliable and ethically responsible machine learning applications.

IV.2.4 Hyperparameters for classification algorithms

After generating the synthetic data, the systematic selection and precise tuning of hyperparameters emerge as a critical factor in guiding the behavior of machine learning models and controlling their learning mechanisms. These hyperparameters directly influence the dynamics of the training process and the model’s ability to extract underlying patterns from the data, which in turn affects prediction accuracy and generalization capability to unseen data.

Moreover, the optimal configuration of hyperparameters contributes to achieving a balanced trade-off between fitting the training data and mitigating the problem of overfitting, thereby ensuring stable and reliable predictive performance. In this context, the set of hyperparameters presented in Table (IV.2) was adopted during the training phase of the proposed model, based on well-defined scientific criteria aimed at maximizing predictive efficiency and attaining optimal model performance.

Table IV.2 Hyperparameters of the AI techniques used

Algorithms	Parameters	Values
DT	Collapse Tree	True
	Confidence factor	0.25
	Num folds	3
	Seedn	1
SVM	SVM Type	C-SVC
	Cache size	40
	Degree	3
	Kernel Type	radial basis function
KNN	K	2
	Search Algorithm	Linear NN Search
AdaBoost	Num Sub Cmtys	1

IV.3 Results and discussion

IV3.1 SHAP-Based Feature Importance and Sample-Level Analysis for DGA Classification

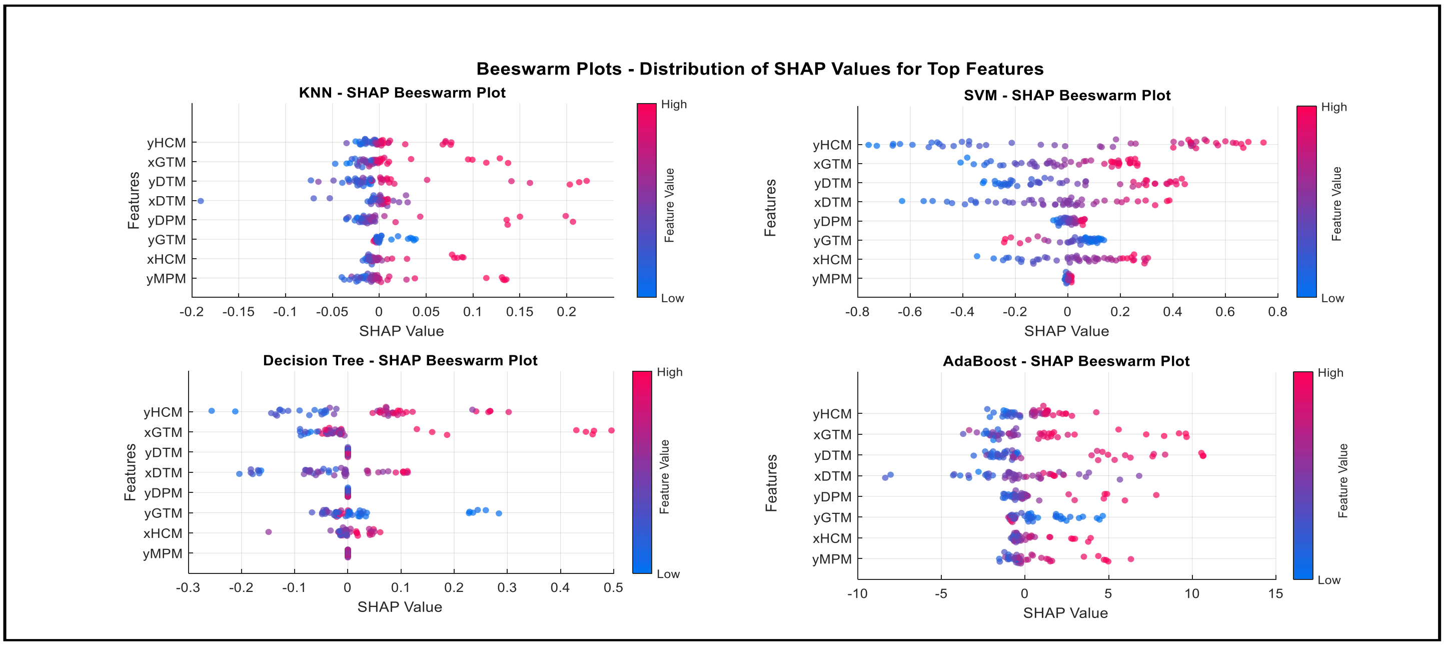

Figure IV.2. Beeswarm Plots - Distribution of SHAP Values for Top Features

Figure IV.2 illustrates the distribution of SHAP values for the most influential features identified in each classification model, highlighting both their relative importance and directional contribution to model predictions. Each point represents an individual observation, with its horizontal position corresponding to the SHAP value and the color gradient representing the feature magnitude, ranging from low (blue) to high (pink). Positive SHAP values indicate a supportive effect on the predicted class, whereas negative values denote an opposing or suppressive influence.

The plots demonstrate that features such as *yHCM, xGTM, yDTM,* and *xDTM* consistently exert substantial impact across all four models, although the magnitude and dispersion of their contributions vary by model type. Specifically, the KNN model exhibits relatively concentrated SHAP values, suggesting moderate, locally distributed effects. In contrast, the SVM model shows broader dispersion, particularly for *yHCM*, reflecting its strong discriminative role. The Decision Tree model presents segmented, threshold-driven distributions, while the AdaBoost model displays the widest SHAP range, indicating amplified feature contributions resulting from the boosting process.

Furthermore, the beeswarm plots provide insights into the relationship between feature magnitude and predictive influence, revealing that higher feature values generally correspond to positive contributions, whereas lower values tend to align with weaker or negative effects. Overall, this analysis underscores the stability of key features across models and demonstrates the effectiveness of SHAP for comparative interpretation of machine-learning predictions.

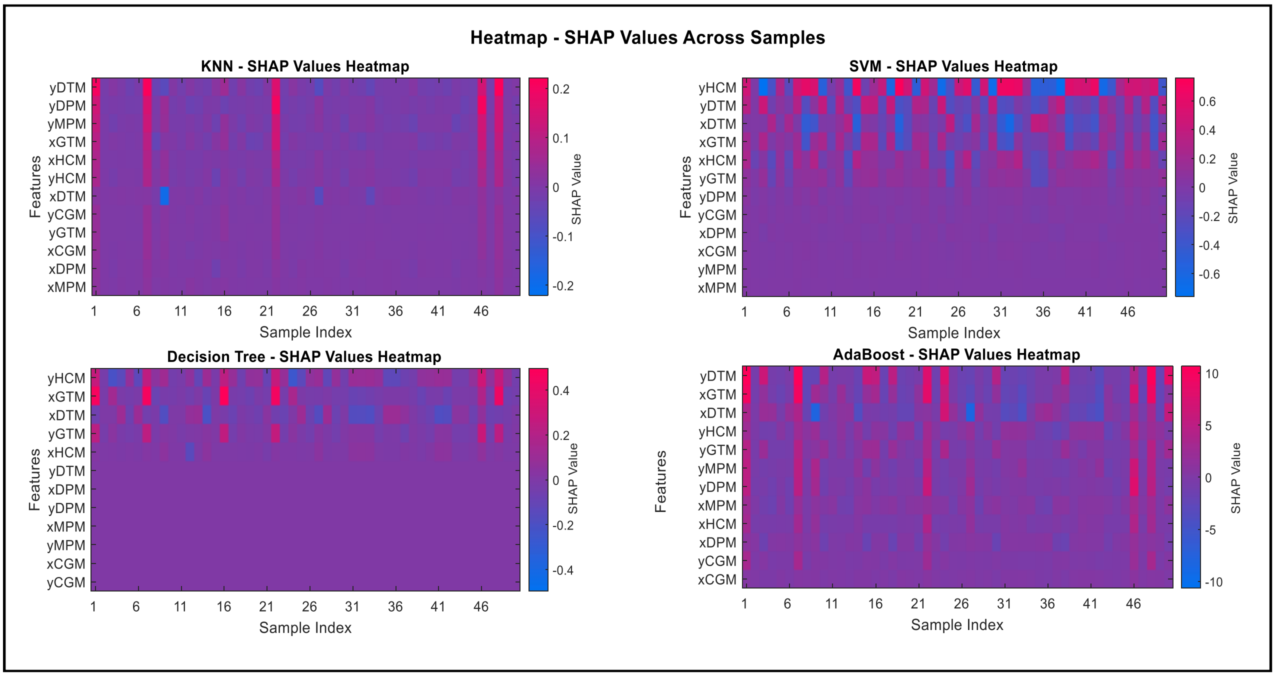

Figure IV.3 Heatmap - SHAP Values Across Samples

Figure IV.3 illustrates the distribution of SHAP values across individual samples for the top features retained in each classification model. The heatmaps offer a compact representation of how feature contributions vary between observations, with color intensity indicating both the magnitude and direction of the SHAP value. Positive SHAP values denote features that increase support for the predicted class, whereas negative values indicate features that reduce support or contribute in the opposite direction.

A general inspection of the heatmaps reveals that feature influence is not uniform across samples, confirming that the predictive role of each variable is sample-dependent rather than constant. Certain features, particularly yDTM, yHCM, xGTM, and xDTM, exhibit repeated bands of higher intensity across multiple models, suggesting a stable and recurrent influence on prediction outcomes. Concurrently, localized regions of high magnitude indicate that specific observations are strongly driven by particular features, highlighting heterogeneity in the classifiers’ decision-making behavior.

Model-specific patterns are also apparent. The KNN heatmap shows relatively moderate SHAP magnitudes concentrated within a narrower range, consistent with the local and distance-based nature of the algorithm. The SVM heatmap demonstrates more structured variation across samples, reflecting stronger discrimination effects for a subset of influential variables. In the Decision Tree model, the contrast between low- and high-contribution regions is more discrete, consistent with the threshold-based partitioning inherent in tree learning. By contrast, the AdaBoost heatmap exhibits the widest dynamic range of SHAP values, reflecting the amplified contribution of certain features through the boosting process.

Overall, these heatmaps complement the beeswarm plots by providing a sample-level perspective on feature interpretation. While beeswarm plots summarize the global distribution of feature effects, the heatmaps reveal where and how these effects manifest across individual observations. This representation thus offers deeper insight into the consistency, variability, and model-specific behavior of the most influential graphical

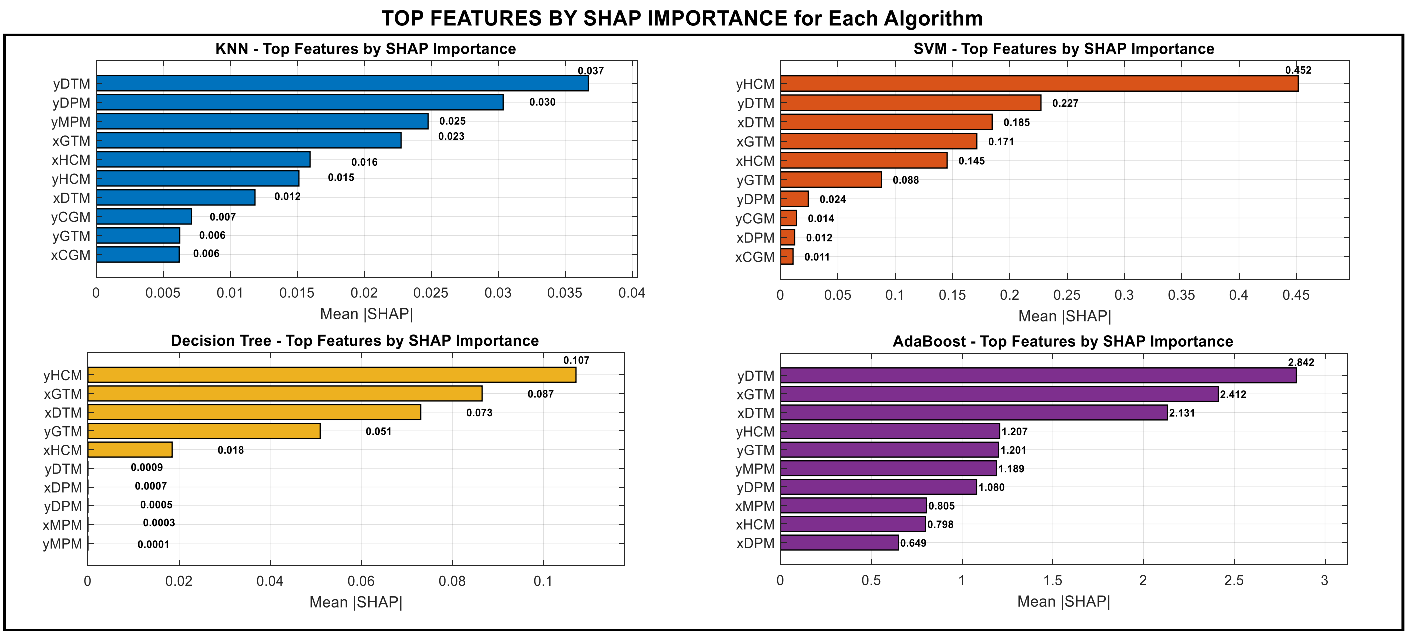

Figure IV.4. Top features ranked by mean absolute SHAP importance for each classification algorithm.

Figure IV.4 presents the ranking of the most influential features for the KNN, SVM, Decision Tree, and AdaBoost models based on the mean absolute SHAP value, which quantifies the average magnitude of each feature's contribution to model predictions. A higher mean |SHAP| value indicates greater overall influence of the corresponding feature on classification outcomes, irrespective of the direction of the effect.

The results reveal that feature importance varies across algorithms, reflecting differences in the internal learning mechanisms of each model. In the KNN classifier, the most influential features are yDTM, yDPM, yMPM, and xGTM, suggesting that this algorithm relies primarily on geometrical descriptors that enhance local similarity-based discrimination. In the SVM model, yHCM emerges as the dominant feature by a substantial margin, followed by yDTM, xDTM, and xGTM, indicating that these variables play a critical role in defining the separating hyperplanes between classes. For the Decision Tree model, importance is concentrated in a smaller subset, with yHCM, xGTM, xDTM, and yGTM showing the highest contributions, while the remaining variables exhibit marginal influence. In the AdaBoost model, the ranking is led by yDTM, xGTM, and xDTM, followed by yHCM and yGTM, highlighting the strong discriminative power of these features within the boosting framework.

A notable observation is the repeated appearance of several variables across all four models, particularly yDTM, xGTM, xDTM, and yHCM. Their recurrence among the top-ranked features indicates that they constitute robust and informative descriptors of the problem domain, maintaining predictive relevance across different classification paradigms. This consistency reinforces their suitability for feature selection and supports their interpretation as core variables in the proposed representation space.

It is also important to note that absolute SHAP magnitudes differ considerably between models, especially in AdaBoost, which exhibits substantially larger values. Consequently, comparisons across algorithms should focus primarily on relative ranking within each model rather than on raw SHAP values. Overall, the figure demonstrates that while each classifier emphasizes features differently, a common subset of graphical descriptors remains consistently influential, underscoring the reliability of the selected feature set.

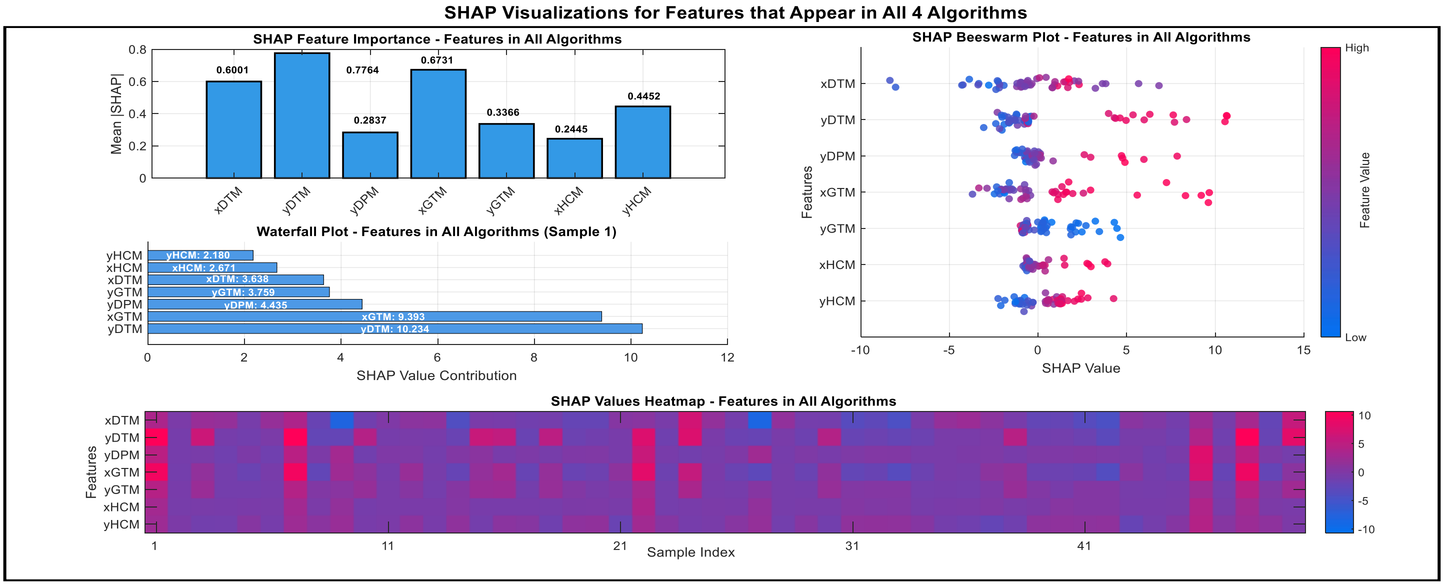

Figure IV.5 SHAP visualizations for the features that consistently appear among the top contributors across all four algorithms.

Figure IV.5 presents an integrated SHAP-based interpretation of the subset of features consistently identified as important by the KNN, SVM, Decision Tree, and AdaBoost models. By focusing exclusively on features shared across all algorithms, the figure highlights the most stable and robust descriptors within the proposed feature space. The combined visualization includes a bar chart of mean absolute SHAP values, a beeswarm plot, a local contribution plot, and a heatmap, providing complementary perspectives on both global and sample-level feature effects.

The upper-left panel summarizes the global importance of the selected features using mean absolute SHAP values. The ranking indicates that xGTM, yDTM, and xHCM are the most influential variables within this consensus feature set, followed by yGTM, xDTM, yDPM, and yHCM. This finding suggests that the retained features preserve substantial explanatory power even when the analysis is restricted to variables exhibiting recurrent importance across all classifiers, reinforcing their relevance as a compact and reliable subset for feature selection.

The upper-right beeswarm plot further refines this interpretation by illustrating the distribution of SHAP values for each retained feature across all analyzed samples. The horizontal spread of points reflects variation in feature influence between observations, while the color gradient represents the magnitude of the underlying feature values. Several features display a structured pattern in which higher feature values correspond to more positive SHAP contributions, whereas lower values are associated with weaker or negative effects. This behavior demonstrates that the selected variables not only rank highly in importance but also exhibit interpretable and systematic relationships with model predictions.

The middle-left local contribution plot emphasizes the relative strength of feature effects for an individual prediction instance. In this panel, yDTM and xGTM make the largest positive contributions, followed by yDPM, yGTM, and xDTM, while yHCM and xHCM contribute less for that specific observation. This confirms that, although all retained features are globally relevant, their local influence may vary considerably between samples, reflecting the context-dependent nature of model explanations.

The lower heatmap extends this analysis to the entire dataset by displaying how SHAP values of the shared features vary across samples. Repeated bands of high and low intensity indicate that certain features exert strong influence for multiple observations, while other regions remain near neutral.

This pattern demonstrates that the selected features maintain predictive relevance across the dataset, albeit with varying strength depending on the specific sample configuration.

Overall, the figure illustrates that the intersection-based feature selection strategy successfully isolates a compact set of features that remain important across fundamentally different learning algorithms. The concordance among global rankings, local contribution patterns, and sample-wise heatmap structures reinforces the interpretability and robustness of the selected features, supporting their use as the final representation for subsequent classification analyses.

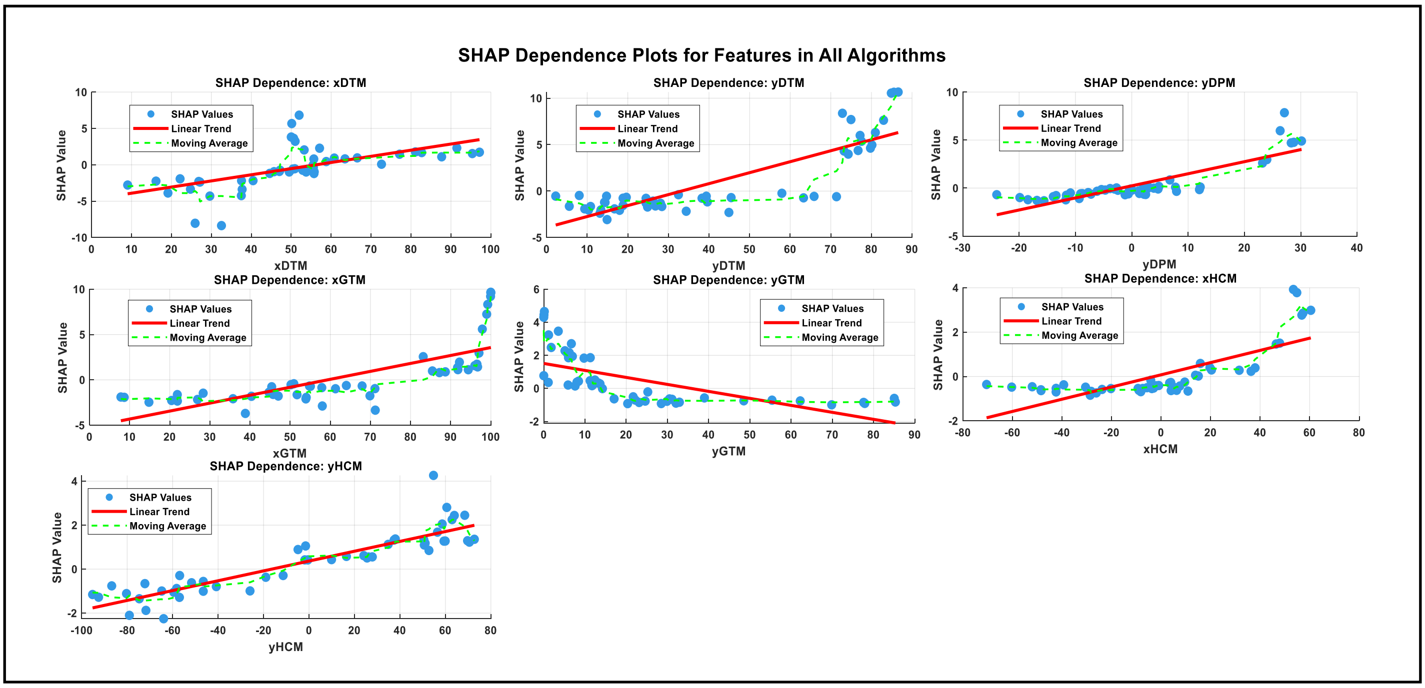

Figure IV.6 SHAP dependence plots for the features retained across all classification algorithms.

Figure IV.6 presents the SHAP dependence plots for the features consistently selected across different classification algorithms, namely KNN, SVM, Decision Tree, and AdaBoost. These plots illustrate the relationship between the actual feature values and their corresponding SHAP values, enabling an analysis of how variations in feature magnitude influence model predictions. Blue points represent individual sample contributions, the red line indicates the global linear trend, and the green dashed curve reflects local behavior based on a moving-average pattern.

The results indicate that the effects of the studied features are partially nonlinear, exhibiting heterogeneous influence patterns. Several variables, including xDTM, yDTM, yDPM, xGTM, xHCM, and yHCM, display a clear increasing trend, suggesting that higher feature values correspond to stronger positive contributions to the prediction, thereby increasing the likelihood of belonging to the target class. The consistency between the global linear trend and the local moving-average curve in these cases supports the presence of a stable monotonic relationship.

In contrast, yGTM exhibits a decreasing pattern, where higher values correspond to lower SHAP contributions, indicating an inverse effect relative to the other features. This behavior may reflect a distinct discriminative role within the adopted feature space.

Additionally, some features show discrepancies between the global linear trend and the local curve, suggesting nonlinear effects or threshold-like behaviors, particularly at higher value ranges. Notably, abrupt changes in SHAP responses are observed for yDTM, xGTM, and yDPM, indicating the existence of critical levels beyond which these features become significantly more influential in the prediction process.

The dispersion of data points around the fitted trends also reflects inter-sample variability, implying that although the overall direction of influence is evident, the magnitude of the effect remains context-dependent. Overall, these dependence plots provide a deeper understanding of the functional relationship between feature values and their predictive contributions. They confirm that the selected features are not only globally important but also exhibit interpretable directional effects, thereby enhancing model interpretability and supporting the robustness and reliability of the final feature subset for accurate classification.

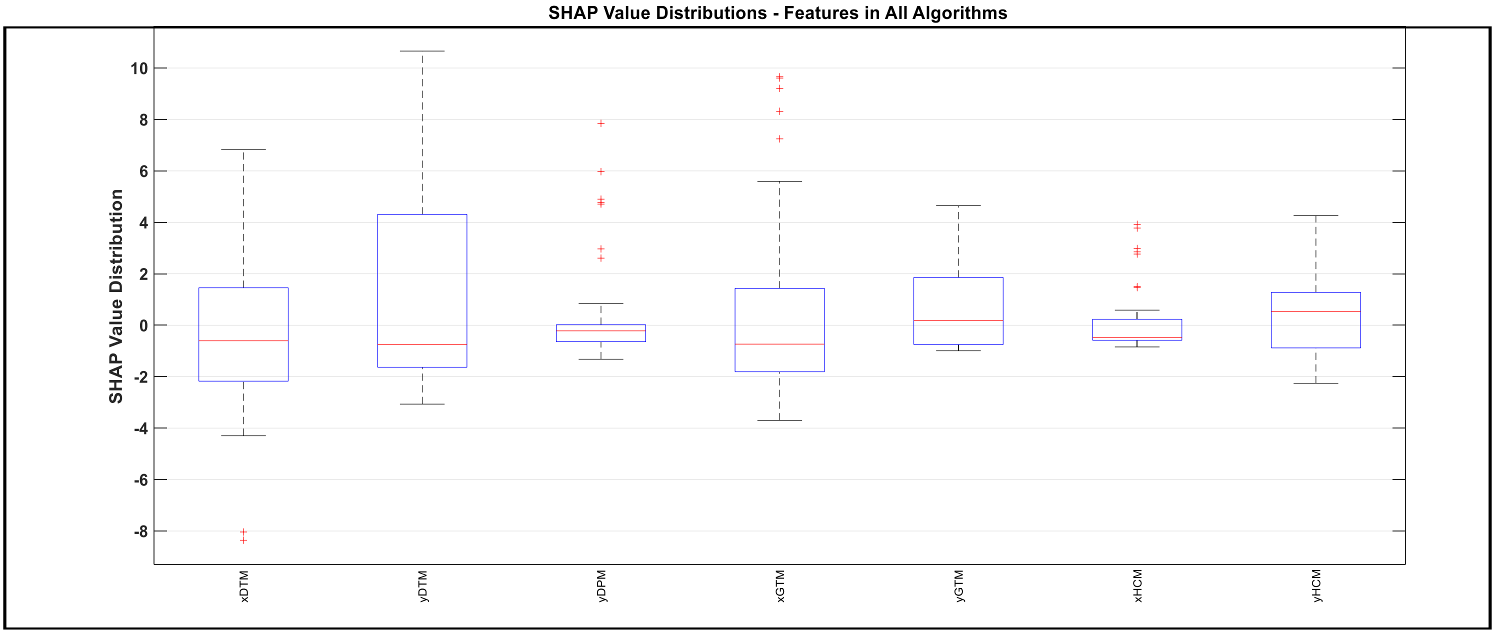

Figure IV.7. SHAP value distributions for the features retained across all algorithms.

Figure IV.7 presents boxplot representations of SHAP value distributions for the features consistently selected by the KNN, SVM, Decision Tree, and AdaBoost models. These boxplots provide a concise summary of the central tendency, dispersion, and presence of outliers in SHAP values, thereby offering insight into how each feature's contribution varies across different samples. The median line within each box represents the typical contribution of a feature, while the interquartile range reflects the variability of its influence. The whiskers and outliers further highlight extreme positive or negative contributions observed in specific cases.

Overall, the figure reveals that the retained features differ not only in their average contribution but also in the stability of their effects across the dataset. Some variables exhibit relatively narrow interquartile ranges with medians close to zero, indicating stable and moderate contributions. In contrast, other features display wider distributions and a higher number of outliers, reflecting greater heterogeneity in their predictive influence. Features with broader distributions tend to play a more variable role in model decisions, contributing significantly in certain instances while remaining less influential in others.

The presence of several high positive outliers suggests that some features can provide strong supportive contributions to the predicted class for specific observations. Conversely, the occurrence of negative outliers indicates that these same features may, in some cases, exert an opposing effect by reducing support for the predicted outcome. This asymmetry confirms that feature effects are context-dependent and vary across samples rather than following a uniform monotonic pattern.

From an interpretative standpoint, these boxplots complement previous SHAP-based visualizations by emphasizing the dispersion characteristics of feature contributions. While bar plots highlight global importance and beeswarm or heatmap representations capture sample-level behavior, the current distributional perspective underscores the degree of consistency or variability associated with each feature. This distinction is particularly valuable for identifying features that are consistently informative versus those whose importance is driven by a limited number of highly influential cases.

In summary, the figure supports the robustness of the final selected feature set while demonstrating that the explanatory contributions of these features are unevenly distributed across observations. This finding underscores the importance of integrating multiple SHAP visualization techniques to achieve a comprehensive understanding of feature behavior within the classification framework.

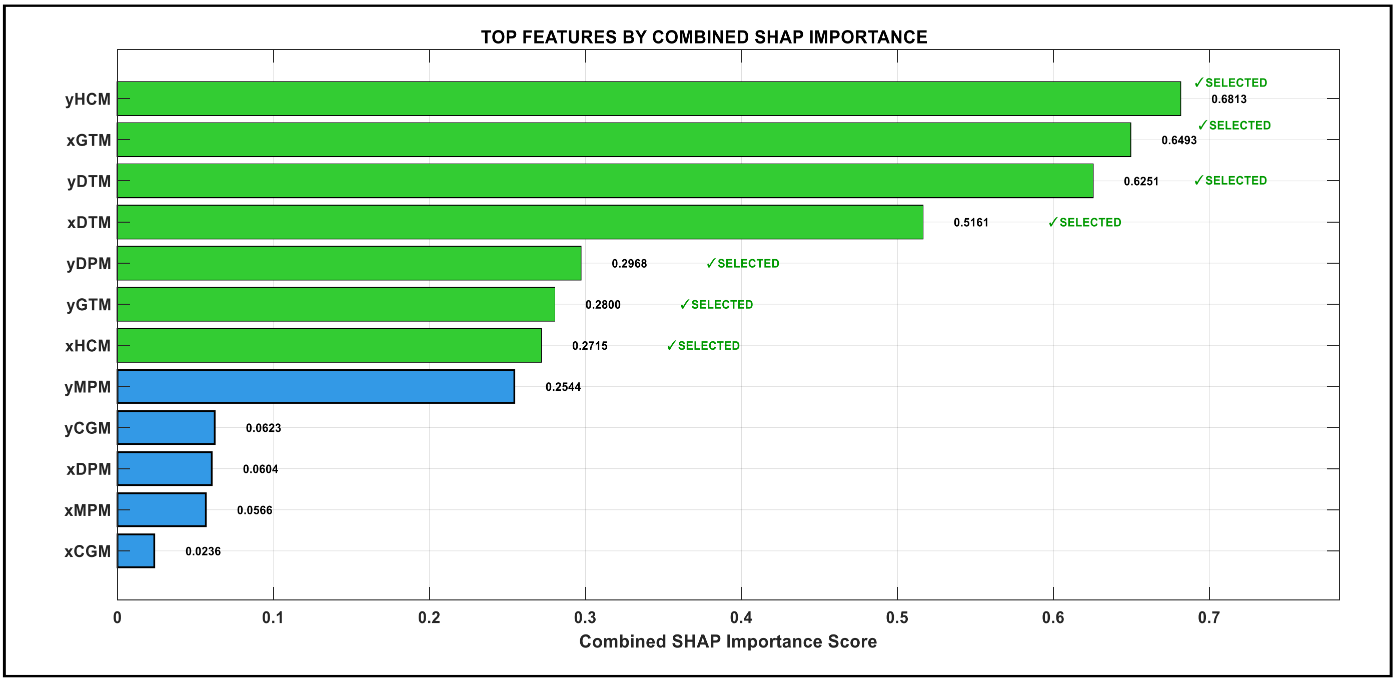

Figure IV.8 Top features ranked by combined SHAP importance score.

Figure IV.8 presents the overall ranking of the extracted features based on the combined SHAP importance score, which is derived by aggregating the normalized SHAP contributions across four classification models, namely KNN, SVM, Decision Tree, and AdaBoost. This approach aims to provide a consensus-based evaluation of feature importance, thereby reducing the bias associated with relying on a single model and enhancing the robustness of the feature selection process. The highlighted features correspond to the final selected subset.

The results indicate that yHCM, xGTM, yDTM, and xDTM occupy the top positions in the ranking, exhibiting significantly higher importance scores compared to the remaining features. This reflects their consistent and substantial contribution to predictive performance across all models. They are followed by yDPM, yGTM, and xHCM, which also demonstrate considerable importance, justifying their inclusion in the selected subset. Collectively, these features form a compact and highly informative representation with strong explanatory power and cross-model consistency.

In contrast, lower-ranked features such as yMPM, yCGM, xDPM, xMPM, and xCGM show relatively low importance scores, indicating limited influence and reduced stability in their contributions when evaluated within a multi-model framework. This disparity highlights the effectiveness of the consensus-based feature selection strategy in distinguishing globally relevant features from those with marginal impact.

An important implication of this figure is that the final feature set is determined based on cross-model agreement rather than isolated importance within a single classifier. This enhances both the interpretability and reliability of the selected features, as they maintain their predictive relevance across different learning mechanisms. Therefore, the combined SHAP framework provides a robust methodological basis for identifying stable features and constructing an efficient low-dimensional representation without compromising essential information.

Overall, Figure IV.8 confirms that the selected feature subset achieves an effective balance between dimensionality reduction and discriminative capability, thereby supporting improved classification performance.

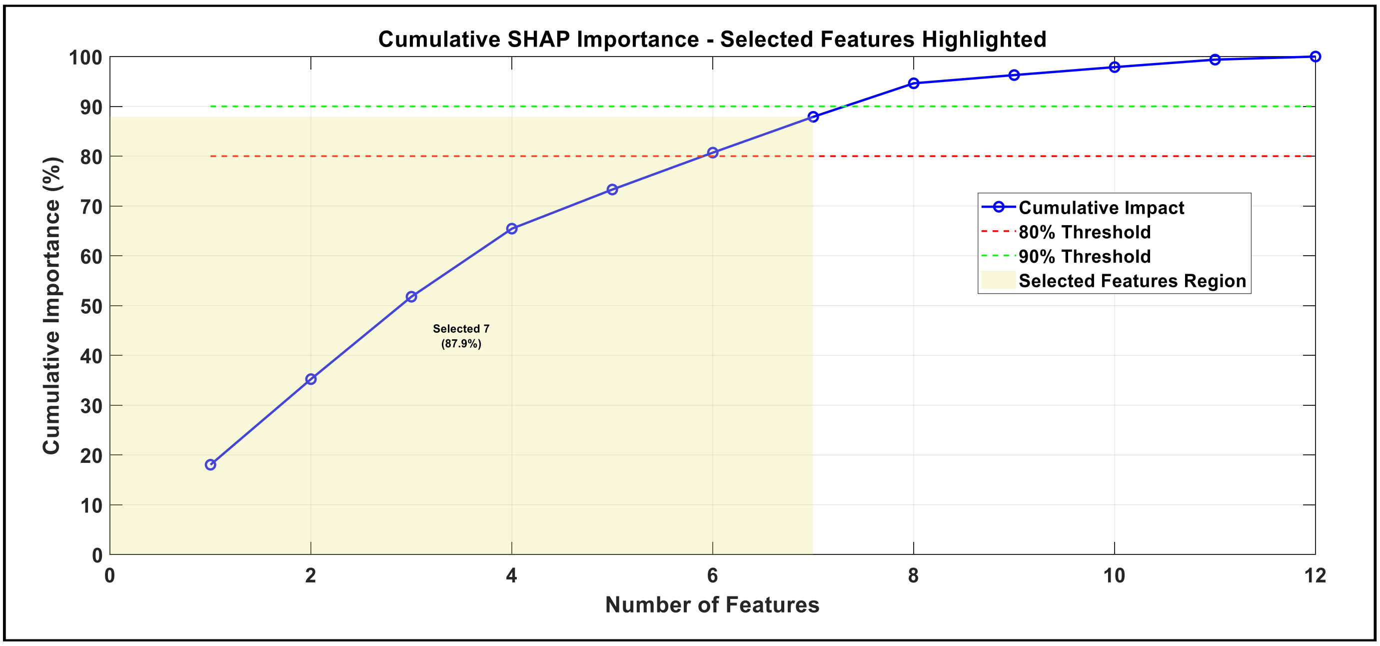

Figure IV.9 Cumulative SHAP importance with the selected features highlighted.

Figure IV.9 illustrates the cumulative contribution of the ranked features to the total combined SHAP importance, providing insight into how explanatory power is progressively accumulated as features are added according to their importance ranking. The blue curve represents the cumulative importance captured by the top-ranked features, while the dashed horizontal lines denote the 80% and 90% importance thresholds. The shaded region highlights the subset of features selected for the final reduced representation.

The curve exhibits a steep initial increase, indicating that a small number of top-ranked features account for a substantial proportion of the total explanatory contribution. In particular, the first seven selected features capture approximately 87.9% of the cumulative importance, exceeding the 80% threshold and approaching the 90% benchmark. This finding demonstrates that the majority of the predictive information is concentrated within a limited subset of features, whereas the remaining variables contribute only marginal additional value.

Furthermore, the shape of the curve reveals a clear diminishing-returns effect. Beyond the selected subset, the slope becomes noticeably flatter, indicating that the inclusion of additional features results in only minor gains in cumulative importance. This behavior confirms that the excluded variables have relatively weak overall influence and further validates the effectiveness of the adopted feature selection strategy. In other words, the

reduced feature set retains most of the relevant explanatory information while avoiding unnecessary dimensional complexity.

From a methodological standpoint, this figure provides strong justification for the selected feature subset. The ability of a compact group of seven features to retain nearly 90% of the total SHAP importance suggests that dimensionality reduction has been achieved without significant loss of predictive or interpretative content. Consequently, the resulting representation offers an effective balance between parsimony and information retention, which is essential for enhancing model interpretability and reducing computational cost.

Overall, Figure IV.9 confirms that the selected features constitute a highly informative subset, capturing the dominant share of cumulative SHAP importance and supporting their use as core descriptors for subsequent classification tasks.

IV.3.2 Model Performance and Classification Evaluation Before and After Feature Selection

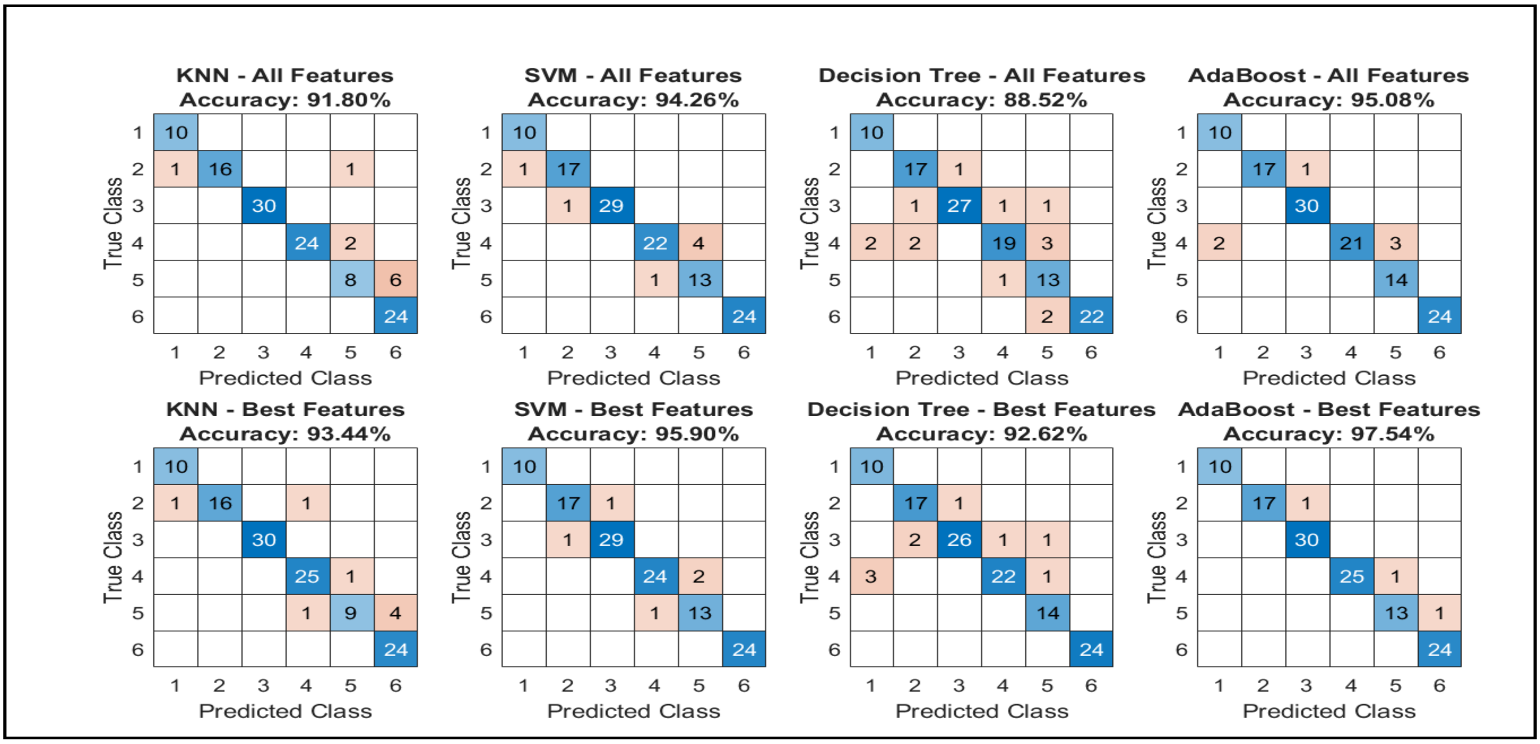

Figure IV.10 Confusion matrices of the four classification models using all features and the selected best features for transformer fault diagnosis (PD = 1, D1 = 2, D2 = 3, T1 = 4, T2 = 5, T3 = 6).

Figure IV.10 presents a comparative analysis of the confusion matrices obtained from the KNN, SVM, Decision Tree, and AdaBoost classifiers before and after feature selection for power transformer fault diagnosis. The six target classes correspond to partial discharge (PD), low-energy discharge (D1), high-energy discharge (D2), low-temperature thermal fault (T1), medium-temperature thermal fault (T2), and high-temperature thermal fault (T3). In each matrix, diagonal elements represent correctly classified instances, while off-diagonal elements indicate misclassifications between fault categories.

Overall, the results demonstrate a consistent improvement in classification performance across all four models following feature selection. When using the full feature set, the achieved accuracies are 91.80% for KNN, 94.26% for SVM, 88.52% for Decision Tree, and 95.08% for AdaBoost. After retaining only the most informative features, the accuracies increase to 93.44%, 95.90%, 92.62%, and 97.54%, respectively. This consistent enhancement confirms that the selected feature subset effectively preserves the most discriminative information while eliminating redundant and less relevant variables.

A detailed examination of the confusion matrices reveals that certain fault categories are more easily distinguishable than others. Specifically, PD (class 1), D2 (class 3), and T3 (class 6) exhibit high classification reliability across most models, as reflected by the strong concentration of values along the main diagonal. In contrast, the most notable misclassifications occur among thermally related faults, particularly between T1 (class 4) and T2 (class 5), and to a lesser extent between adjacent discharge-related classes such as PD (class 1) and D1 (class 2). This behavior is expected in transformer fault diagnosis, as similar thermal or discharge conditions may produce partially overlapping gas pattern characteristics.

Among the evaluated classifiers, AdaBoost achieves the best overall performance both before and after feature selection, reaching the highest final accuracy of 97.54%. Its post-selection confusion matrix exhibits the strongest diagonal dominance and the lowest number of misclassifications, indicating superior discriminative capability among the six fault classes. The SVM model also demonstrates strong performance, with minimal confusion and a final accuracy of 95.90%. KNN provides satisfactory results, although some residual confusion persists between neighboring classes. Notably, the Decision Tree model shows the most significant improvement after feature selection, suggesting that it benefits considerably from the removal of less informative features and the focus on the most relevant descriptors.

In summary, Figure IV.10 highlights the effectiveness of the proposed SHAP-based feature selection strategy in enhancing class separability and improving classification consistency across all models. The results further indicate that AdaBoost and SVM are particularly well-suited for accurately distinguishing between transformer fault conditions represented by PD, D1, D2, T1, T2, and T3.

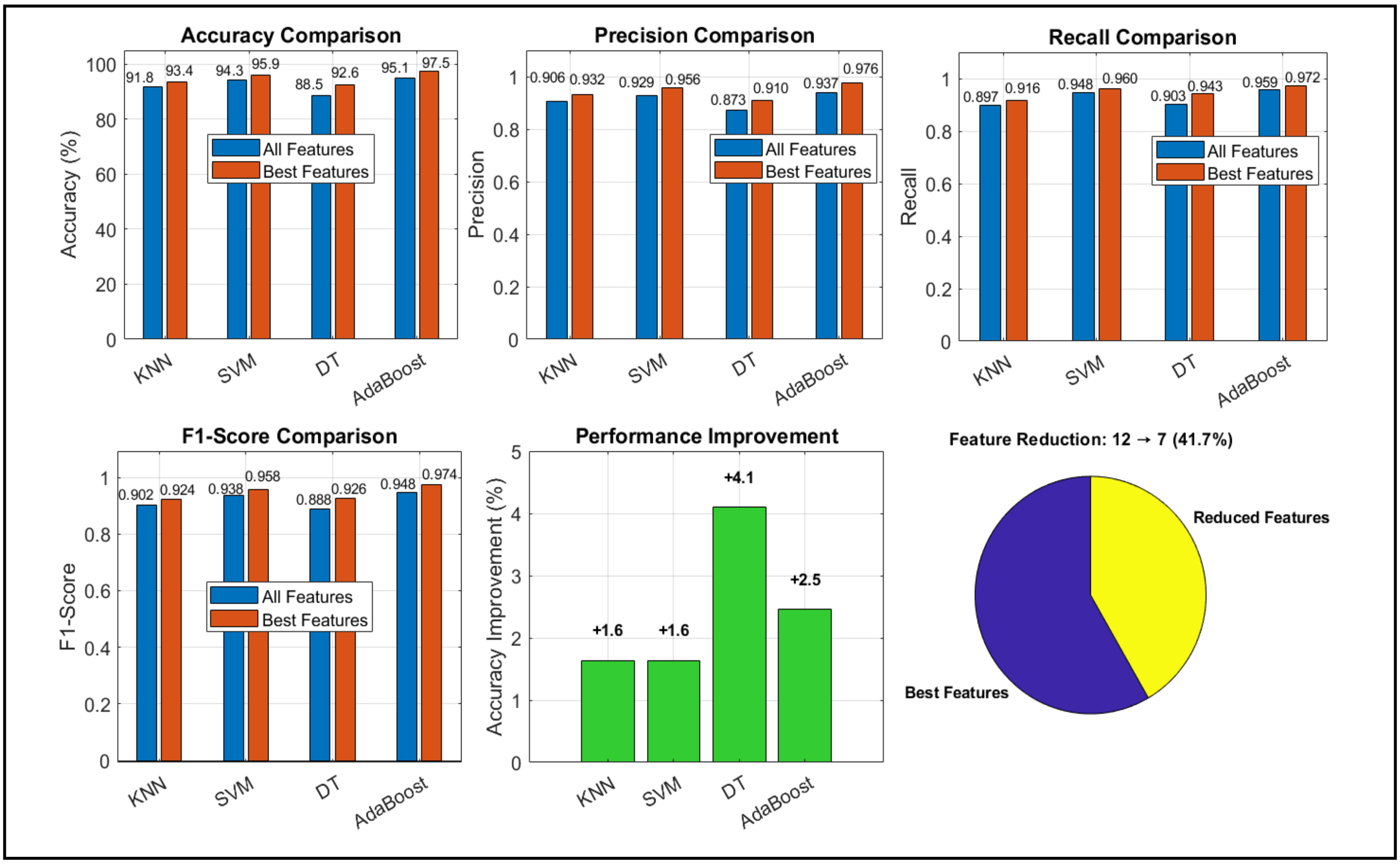

Figure IV.11 Performance metrics comparison of the classification models before and after feature selection.

Figure IV.11 presents a comparative evaluation of the predictive performance of the KNN, SVM, Decision Tree, and AdaBoost classifiers using both the full feature set and the selected subset of optimal features. The comparison is based on four standard evaluation metrics—accuracy, precision, recall, and F1-score—along with the corresponding improvement in accuracy and the degree of feature reduction achieved through SHAP-based feature selection.

The results indicate that feature selection leads to a consistent improvement across all performance metrics and for all classifiers. In terms of accuracy, KNN improves from 91.8% to 93.4%, SVM from 94.3% to 95.9%, Decision Tree from 88.5% to 92.6%, and AdaBoost from 95.1% to 97.5%. Similar enhancements are observed in precision, recall, and F1-score, demonstrating that the selected feature subset not only increases the proportion of correctly classified instances but also improves the balance between false positives and false negatives. These findings confirm that the retained features effectively capture the most discriminative information while eliminating redundant or less informative variables.

Among the evaluated models, AdaBoost achieves the best overall performance after feature selection, reaching an accuracy of 97.5%, precision of 0.976, recall of 0.972, and F1-score of 0.974, indicating superior robustness and discriminative capability. The SVM model also maintains strong performance, while KNN shows moderate yet consistent improvements. Notably, the Decision Tree classifier exhibits the largest relative gain in accuracy, with an increase of approximately 4.1 percentage points, suggesting that it benefits significantly from dimensionality reduction and noise elimination. In comparison, KNN and SVM achieve smaller but meaningful improvements of around 1.6 percentage points, while AdaBoost improves by approximately 2.5 percentage points.

Overall, Figure IV.11 demonstrates that the proposed SHAP-based feature selection approach enhances classification performance while reducing feature dimensionality. This confirms the effectiveness of the selected feature subset in achieving a favorable trade-off between model accuracy, robustness, and computational efficiency.

Table IV.3 Importance of Features Derived from DGA Graphical Techniques

Features	**Percentage 1**	**Percentage2**
F1	50 %	100 %
F2	50%	
F3	50%	100 %
F4	50%	
F5	0 %	50 %
F6	50 %	
F7	0 %	0 %
F8	0 %	
F9	0 %	0 %
F10	0 %	
F11	50 %	100 %
F12	50 %	

The analysis of **Table (IV.3)** highlights the significance of the different graphical methods used in **Dissolved Gas Analysis (DGA)** through the evaluation of the features extracted from them. The results indicate that some diagnostic methods provide more informative representations of gas behavior in transformer oil, making them more reliable for identifying fault types.

Among these methods, the **Duval Triangle method** stands out as one of the most widely used techniques for transformer fault diagnosis due to its ability to effectively distinguish between major fault categories such as partial discharges, thermal faults, and electrical arcing. In addition, the **Duval Pentagon method** offers a more detailed diagnostic capability in certain complex cases, as it relies on a larger set of gases and represents them within a more comprehensive geometric diagram.

Other methods, such as the **Gouda Triangle** and the **Mansour Pentagon**, also contribute to enhancing the diagnostic capability of traditional approaches by providing alternative geometric representations of gas distributions, which can help interpret cases that may not be clearly identified using a single method. Furthermore, the **Circle Method** provides another geometric representation based on circular mapping of gas concentrations, allowing relationships among gases to be analyzed from a different perspective that supports the diagnostic process.

Overall, the analysis of the table indicates that methods based on the **geometric representation of gas ratios** are among the most effective approaches for interpreting DGA data. Moreover, the findings suggest that relying on **multiple graphical methods simultaneously** can provide a more comprehensive understanding of gas behavior within transformer oil, thereby improving the accuracy of fault diagnosis and enhancing the reliability of transformer monitoring and maintenance systems

IV.4 Conclusion

This chapter presented a comprehensive experimental evaluation of the proposed artificial intelligence–based framework for power transformer fault diagnosis using Dissolved Gas Analysis (DGA). Advanced machine learning techniques were integrated with SHAP-based feature selection to enhance both predictive performance and model interpretability, which are essential components of reliable industrial decision-support systems.

The results demonstrated that the use of SHAP enabled the identification of a compact and highly informative subset of features, leading to effective dimensionality reduction without loss of critical information. This process significantly improved model performance while maintaining the most discriminative characteristics of the data. The consistency of key features across different algorithms further confirmed the robustness of the proposed feature representation.

A comparative analysis of classification algorithms—KNN, SVM, Decision Tree (DT), and AdaBoost—revealed a general improvement in all evaluation metrics after feature selection. AdaBoost achieved the highest overall performance, while the Decision Tree model exhibited the most significant relative improvement, highlighting the importance of reducing noise and focusing on the most relevant features.

Furthermore, the various SHAP-based visual analyses provided deep insights into model behavior at both global and local levels, thereby enhancing the transparency and reliability of the proposed system and supporting its applicability in real-world scenarios.

In addition, the results showed that graphical methods used in DGA, particularly those based on the geometric representation of gas ratios, play a crucial role in improving diagnostic accuracy. Some methods demonstrate strong capability in distinguishing between major fault types, while others provide complementary representations that help interpret more complex cases. This confirms that combining multiple graphical approaches offers a more comprehensive understanding of gas behavior in transformer oil, ultimately improving the accuracy and reliability of the diagnostic process.

In conclusion, the proposed methodology proves effective in achieving a balance between accuracy, robustness, and interpretability by integrating explainable artificial intelligence techniques with advanced geometric representations of DGA data. These findings open promising perspectives for future research aimed at developing more efficient and real-time intelligent systems for power transformer monitoring and maintenance.

Conclusion

Conclusion

This study has provided a comprehensive comparative analysis of graphical fault detection methods for power transformers using Dissolved Gas Analysis (DGA), enhanced with modern artificial intelligence techniques. The results indicate that graphical methods such as the **Duval Triangle**, renowned for its ability to differentiate between major fault types—including partial discharges, thermal faults, and electrical arcing—remain among the most widely used and effective diagnostic tools. Methods such as the **Duval Pentagon**, **Gouda Triangle**, **Mansour Pentagon**, and **Circle Method** further enrich the diagnostic process by providing alternative geometric representations of gas concentrations, enabling the interpretation of complex cases that may not be clearly identified by a single method.

The study demonstrates that integrating these multiple graphical approaches with artificial intelligence models, including SVM, AdBoost, KNN, and ensemble algorithms, significantly enhances fault diagnosis accuracy and enables predictive maintenance, thereby reducing operational risks. Performance metrics such as Accuracy, Recall, F1-Score, and AUC provided a comprehensive evaluation of the diagnostic models, confirming the strength of the integrated approach combining graphical analysis and AI.

In conclusion, this research confirms that employing multiple graphical fault detection methods, supported by machine learning and intelligent data analysis, not only improves the diagnostic precision for power transformers but also establishes a robust foundation for developing intelligent monitoring systems capable of effective predictive maintenance. This approach ensures operational reliability and sustainability of electrical networks, positioning this work as a strategic and promising contribution to the field of smart energy systems.

References

[1] J. Faiz and B. M. Ebrahimi, "Transformer fault diagnosis based on dissolved gas analysis: A review," IET Electric Power Applications, vol. 5, no. 1, pp. 1–11, 2011.

[2] M. Duval, "A review of faults detectable by gas-in-oil analysis in transformers," IEEE Electrical Insulation Magazine, vol. 18, no. 3, pp. 8–17, 2002.

[3] Z. Wang, Y. Liu, and P. Griffin, "Neural network-based fault diagnosis of power transformers using dissolved gas analysis," IEEE Transactions on Power Delivery, vol. 16, no. 2, pp. 199–204, 2001.

[4] S. V. Kulkarni and S. A. Khaparde, Transformer Engineering: Design and Practice. New York, NY, USA: Marcel Dekker, 2004.

[5] S. V. Kulkarni and S. A. Khaparde, Transformer Engineering: Design and Practice. New York, NY, USA: Marcel Dekker, 2004.

[6] A. E. Fitzgerald, C. Kingsley Jr., and S. D. Umans, Electric Machinery, 6th ed. New York, NY, USA: McGraw-Hill, 2003.

[7] IEC 60076-1:2011, Power Transformers – Part 1: General. Geneva, Switzerland: International Electrotechnical Commission (IEC), 2011.

[8] A. Leksir, "Synthesis of techniques used for diagnosing faults in electric machines," Ph.D. dissertation, Badji Mokhtar–Annaba University, Annaba, Algeria, 2020.

[9] IEC 60599:2015, Mineral Oil-Filled Electrical Equipment in Service – Guidance on the Interpretation of Dissolved and Free Gases Analysis. Geneva, Switzerland: International Electrotechnical Commission (IEC), 2015.

[10] A. Bourgeois, "Etude du phénomène d'électrisation par écoulement sur les cartons des transformateurs de puissance," Mémoire, Institut National Polytechnique de Grenoble, Grenoble, France, Feb. 2007.

[11] IEEE Std C57.104-2019, IEEE Guide for the Interpretation of Gases Generated in Mineral Oil-Immersed Transformers. Piscataway, NJ, USA: IEEE Power & Energy Society, Nov. 2019.

References

[12] J. Sanchez, "Aide au diagnostic de défauts des transformateurs de puissance," Université de Grenoble, Grenoble, France, 2011.

[13] B. Ahmed and M. Hocine, "Application de méthodes intelligentes pour le diagnostic de l'huile de transformateur par analyse des gaz dissous."

[14] R. Minkner and J. Schmid, The Technology of Instrument Transformers.

[15] S. A. Wani, "Transformer Fault Diagnosis Based on Dissolved Gas Analysis (DGA)."

[16] K. F. Thang, An Improved Approach to Data Analysis and Interpretation in Transformer Condition Assessment Based on Unsupervised Neural Network. University of Bath, United Kingdom, 2002.

[17] S. Li, "Study of Dissolved Gas Analysis under Electrical and Thermal Stresses for Natural Esters Used in Power Transformers," The University of Manchester, United Kingdom, 2012.

[18] Y. Li, "The State of the Art in Transformer Fault Diagnosis with Artificial Intelligence and Dissolved Gas Analysis: A Review of the Literature," arXiv preprint arXiv:2304.11880, 2023.

[19] A. Ahmed, Power Transformer Condition Monitoring and Diagnosis. United Kingdom: The Institution of Engineering and Technology (IET), 2018.

[20] J. Ni, Z. Zhao, S. Tan, Y. Chen, C. Yao, and C. Tang, "The actual measurement and analysis of transformer winding deformation fault degrees by FRA using mathematical indicators," Electric Power Systems Research, vol. 184, p. 106324, 2020, doi: 10.1016/j.epsr.2020.106324.

[21] S. X. Qian, Q. Du, X. J. Gu, and J. Y. Song, "Transformer Winding Deformation Fault Diagnose Based on FRA and Energy Feature Extraction by Wavelet Packet," Advanced Materials Research, vol. 490–495, pp. 1486–1490, 2012, doi:10.4028/www.scientific.net/AMR.490-495.1486.

[22] T.-D. Do, V.-N. Tuyet-Doan, Y.-S. Cho, J.-H. Sun, and Y.-H. Kim, "Convolutional-Neural-Network-Based Partial Discharge Diagnosis for Power Transformer Using UHF Sensor," IEEE Access, vol. 8, pp. 207377–207388, 2020, doi:10.1109/ACCESS.2020.3038386.

[23] H. Karami, H. Tabarsa, G. B. Gharehpetian, Y. Norouzi, and M. A. Hejazi, "Feasibility Study on Simultaneous Detection of Partial Discharge and Axial Displacement of HV Transformer Winding Using

Electromagnetic Waves," IEEE Transactions on Industrial Informatics, vol. 16, no. 1, pp. 67–76, 2019, doi:10.1109/TII.2019.2915685.

[24] A. Indarto, A. W. Murti, F. Husnayain, I. Garniwa, A. Rahardjo, and C. Hudaya, "Influence of Different Adhesives on Partial Discharge in Power Transformer Winding Cylinder Insulation," IEEE Transactions on Dielectrics and Electrical Insulation, vol. 27, no. 3, pp. 964–970, 2020, doi:10.1109/TDEI.2020.008533.

[25] Y. Shi, S. Ji, F. Zhang, Y. Dang, and L. Zhu, "Application of Operating Deflection Shapes to the Vibration-Based Mechanical Condition Monitoring of Power Transformer Windings," IEEE Transactions on Power Delivery, vol. 36, no. 4, pp. 2164–2173, 2020, doi:10.1109/TPWRD.2020.3021909.

[26] H. Zhou, K. Hong, H. Huang, and J. Zhou, "Transformer Winding Fault Detection by Vibration Analysis Methods," Applied Acoustics, vol. 114, pp. 136–146, 2016, doi: 10.1016/j.apacoust.2016.07.024.

[27] Y. Zhou et al., "Vibration Signal-Based Fusion Residual Attention Model for Power Transformer Fault Diagnosis," IEEE Sensors Journal, vol. 24, no. 10, pp. 17231–17242, 2024, doi:10.1109/JSEN.2024.3382811.

[28] L. Jin, D. Kim, A. Abu-Siada, and S. Kumar, "Oil-Immersed Power Transformer Condition Monitoring Methodologies: A Review," Energies, vol. 15, no. 9, p. 3379, 2022, doi:10.3390/en15093379.

[29] N. A. Baka, A. Abu-Siada, S. Islam, and M. El-Naggar, "A New Technique to Measure Interfacial Tension of Transformer Oil Using UV-Vis Spectroscopy," IEEE Transactions on Dielectrics and Electrical Insulation, vol. 22, no. 2, pp. 1275–1282, 2015, doi:10.1109/TDEI.2015.7076831.

[30] H. Torkaman and F. Karimi, "Measurement Variations of Insulation Resistance/Polarization Index During Utilizing Time in HV Electrical Machines – A Survey," Measurement, vol. 59, pp. 21–29, 2015, doi:10.1016/j.measurement.2014.09.034.

[31] T. Mariprasath and V. Kirubakaran, "A Real Time Study on Condition Monitoring of Distribution Transformer Using Thermal Imager," Infrared Physics & Technology, vol. 90, pp. 78–86, 2018, doi: 10.1016/j.infrared.2018.02.009.

[32] F. Segovia et al., "Connected System for Monitoring Electrical Power Transformers Using Thermal Imaging," Integrated Computer-Aided Engineering, vol. 30, no. 4, pp. 353–368, 2023, doi:10.3233/ICA-230712.

References

[33] A. Abdali, A. Abedi, H. Masoumkhani, K. Mazlumi, A. Rabiee, and J. M. Guerrero, "Magnetic-Thermal Analysis of Distribution Transformer: Validation via Optical Fiber Sensors and Thermography," International Journal of Electrical Power & Energy Systems, vol. 153, p. 109346, 2023, doi: 10.1016/j.ijepes.2023.109346.

[34] J. Lukic et al., "Changes of New Unused Insulating Kraft Paper Properties During Drying—Impact on Degree of Polymerization," Electra (Paris), no. 312, pp. 76–81, 2020.

[35] S. Gao, L. Yang, and T. Ke, "Failure Mechanism of Transformer Oil-Immersed Cellulosic Insulation Induced by Sulfur Corrosion," Cellulose, vol. 27, no. 12, pp. 7157–7174, 2020, doi:10.1007/s10570-020-03271-x.

[36] A. Kumar, D. Mishra, and A. Baral, "Importance of Depolarization Current in the Diagnosis of Oil-Paper Insulation of Power Transformer," IEEE Access, vol. 11, pp. 56858–56864, 2023, doi:10.1109/ACCESS.2023.3283914.

[37] D. Mishra, A. Baral, and S. Chakravorti, "Reliable Assessment of Oil-Paper Insulation Used in Power Transformer Using Concise Dielectric Response Measurement," IEEE Transactions on Dielectrics and Electrical Insulation, vol. 30, no. 3, pp. 1255–1264, 2023, doi:10.1109/TDEI.2023.3261824.

[38] B. Standard, "Insulating Liquids—Determination of Breakdown Voltage at Power Frequency—Test Method," BS EN 60156, 1996.

[39] M. R. Mahmoudi, M. H. Heydari, and R. Roohi, "A New Method to Compare the Spectral Densities of Two Independent Periodically Correlated Time Series," Mathematics and Computers in Simulation, vol. 160, pp. 103–110, 2019, doi: 10.1016/j.matcom.2018.12.008.

[40] I. Fofana, A. Bouaicha, and M. Farzaneh, "Characterization of Aging Transformer Oil–Pressboard Insulation Using Some Modern Diagnostic Techniques," European Transactions on Electrical Power, vol. 21, no. 1, pp. 1110–1127, 2011, doi:10.1002/etep.499.

[41] J. S. N'Cho, I. Fofana, Y. Hadjadj, and A. Beroual, "Review of Physicochemical-Based Diagnostic Techniques for Assessing Insulation Condition in Aged Transformers," Energies, vol. 9, no. 5, p. 367, 2016, doi:10.3390/en9050367.

References

[42] M. R. Mahmoudi, M. Mahmoudi, and E. Nahavandi, "Testing the Difference Between Two Independent Regression Models," Communications in Statistics—Theory and Methods, vol. 45, no. 21, pp. 6284–6289, 2016, doi:10.1080/03610926.2014.960584.

[43] A. R. Abbasi, "Fault Detection and Diagnosis in Power Transformers: A Comprehensive Review and Classification of Publications and Methods," Electric Power Systems Research, vol. 209, p. 107990, 2022, doi: 10.1016/j.epsr.2022.107990.

[44] S. Pramanik, V. C. Duvvury, and S. Sahoo, "Tank Current Measurement of Three-Phase Transformer: Its Resonance Behavior and Sensitivity to Detect Mechanical Faults," IEEE Transactions on Power Delivery, vol. 34, no. 6, pp. 2211–2218, 2019, doi:10.1109/TPWRD.2019.2914249.

[45] Z. Zhao, C. Yao, C. Li, and S. Islam, "Detection of Power Transformer Winding Deformation Using Improved FRA Based on Binary Morphology and Extreme Point Variation," IEEE Transactions on Industrial Electronics, vol. 65, no. 4, pp. 3509–3519, 2017, doi:10.1109/TIE.2017.2752135.

[46] S. Gajbhiye, "Detection of Incipient Faults in Transformer by Dissolved Gas Analysis Using Artificial Intelligence Techniques," SSRN Electronic Journal, 2023, doi:10.2139/ssrn.4344852.

[47] S. Singh and M. Bandyopadhyay, "Dissolved Gas Analysis Technique for Incipient Fault Diagnosis in Power Transformers: A Bibliographic Survey," IEEE Electrical Insulation Magazine, vol. 26, no. 6, pp. 41–46, 2010, doi:10.1109/MEI.2010.5599978.

[48] J. Faiz and M. Soleimani, "Assessment of Computational Intelligence and Conventional Dissolved Gas Analysis Methods for Transformer Fault Diagnosis," IEEE Transactions on Dielectrics and Electrical Insulation, vol. 25, no. 5, pp. 1798–1806, 2018, doi:10.1109/TDEI.2018.007191.

[49] H. G. Zaini, "Diagnosis of the Power Transformer Faults Based on DGA Using Intelligent Classifier," International Journal of Engineering Research and Technology, vol. 12, no. 11, pp. 1964–1971, 2019.

[50] J. Rodríguez, J. Contreras, and C. Gaytán, "Evaluation and Interpretation of Dissolved Gas Analysis of Soybean-Based Natural Ester Insulating Liquid," IEEE Transactions on Dielectrics and Electrical Insulation, vol. 28, no. 4, pp. 1343–1348, 2021, doi:10.1109/TDEI.2021.009467.

[51] N. S. N. Klairuang, "Condition Assessment of Oil-Impregnated Paper Insulation of Transformers by Using CFA Index and Degree of Polymerization."

References

[52] M. Buchholz, "The Buchholz Protection System and Its Application in Practice," ETZ, vol. 49, no. 34, pp. 1257–1262, 1928.

[53] S. D. Myers, J. J. Kelly, and R. H. Parrish, A Guide to Transformer Maintenance. Transformer Maintenance Institute, 1981.

[54] J. J. Kelly, "Transformer Fault Diagnosis by Dissolved-Gas Analysis," IEEE Transactions on Industry Applications, no. 6, pp. 777–782, 1980, doi:10.1109/TIA.1980.4503871.

[55] IEC 60567:2011, Oil-Filled Electrical Equipment—Sampling of Gases and Analysis of Free and Dissolved Gases—Guidance. Geneva, Switzerland: International Electrotechnical Commission, 2011.

[56] B. Vahidi and A. Teymouri, Quality Confirmation Tests for Power Transformer Insulation Systems. Cham, Switzerland: Springer, 2019.

[57] N. A. Bakar, A. Abu-Siada, and S. Islam, "A Review of Dissolved Gas Analysis Measurement and Interpretation Techniques," IEEE Electrical Insulation Magazine, vol. 30, no. 3, pp. 39–49, 2014, doi:10.1109/MEI.2014.6804740.

[58] A. Krontiris, "Fuzzy Systems for Condition Assessment of Equipment in Electric Power Systems," 2012.

[59] E. Hubacher, "Analysis of Dissolved Gas in Transformer Oil to Evaluate Equipment Condition," in PCEA Engineering and Operation Section Spring Conference, 1976.

[60] A. Mollmann and B. Pahlavanpour, "New Guidelines for Interpretation of Dissolved Gas Analysis in Oil-Filled Transformers," Electra, vol. 186, pp. 31–51, 1999.

[61] B. Fallou, "Detection of and Research for the Characteristics of an Incipient Fault from Analysis of Dissolved Gases in the Oil of an Insulation," Electra, vol. 42, no. 3, pp. 31–52, 1975.

[62] S. Babukutty and S. Khule, "Combined Dissolved Gas Analysis: A Prescient Methodology for Recognizing Faults in Transformer by MATLAB GUI," International Research Journal of Engineering and Technology (IRJET), 2019.

References

[63] IEC 599, Interpretation of the Analysis of Gases in Transformers and Other Oil-Filled Electrical Equipment in Service. Geneva, Switzerland: International Electrotechnical Commission, 1978.

[64] L. Cheng and T. Yu, "Dissolved Gas Analysis Principle-Based Intelligent Approaches to Fault Diagnosis and Decision Making for Large Oil-Immersed Power Transformers: A Survey," Energies, vol. 11, no. 4, p. 913, 2018, doi:10.3390/en11040913.

[65] S. EE, "46.501: Diagnosis Oil-Filled Transformer Equipment Based on the Results of Chromatographic Analysis of Free Gas Selected with Gas Relay and Gases Dissolved in Insulating Oil," Kyiv, Ukraine, 2007.

[66] O. Shutenko and O. Kulyk, "Comparative Analysis of New Methods for Defect Type Recognition by Dissolved Gas Analysis," in 2022 IEEE 3rd KhPI Week on Advanced Technology (KhPIWeek), 2022, pp. 1–6, doi:10.1109/KhPIWeek57572.2022.9916319.

[67] S.-W. Kim, S.-J. Kim, H.-D. Seo, J.-R. Jung, H.-J. Yang, and M. Duval, "New Methods of DGA Diagnosis Using IEC TC 10 and Related Databases Part 1: Application of Gas-Ratio Combinations," IEEE Transactions on Dielectrics and Electrical Insulation, vol. 20, no. 2, pp. 685–690, 2013, doi:10.1109/TDEI.2013.6508773.

[68] O. E. Gouda, S. H. El-Hoshy, and H. H. El-Tamaly, "Proposed Three Ratios Technique for the Interpretation of Mineral Oil Transformers Based Dissolved Gas Analysis," IET Generation, Transmission & Distribution, vol. 12, no. 11, pp. 2650–2661, 2018, doi:10.1049/iet-gtd.2017.1927.

[69] A. Nanfak, C. H. Kom, and S. Eke, "Hybrid Method for Power Transformers Faults Diagnosis Based on Ensemble Bagged Tree Classification and Training Subsets Using Rogers and Gouda Ratios," International Journal of Intelligent Engineering and Systems, vol. 15, no. 5, 2022, doi:10.22266/ijies2022.1031.02.

[70] M. Duval, "Fault Gases Formed in Oil-Filled Breathing EHV Power Transformers—Interpretation of Gas Analysis Data," IEEE Transactions on Power Apparatus and Systems, no. 6, pp. 1745–1746, 1974.

[71] O. S. Kulyk, "Analysis of the Diagnostic Criteria Used for Defect Type Recognition Based on the Results of Analysis of Gases Dissolved in Oil," Bulletin of the National Technical University 'KhPI', no. 1, pp. 15–25, 2020, doi:10.20998/2224-0349.2020.01.03.

References

[72] A. Gupta, K. Jain, Y. R. Sood, and N. K. Sharma, "Comparative Study of Duval Triangle with the New DGA Interpretation Scheme," in Advances in System Optimization and Control: Select Proceedings of ICAEDC 2017, Springer, 2018, pp. 261–268.

[73] M. S. Ali, A. Omar, A. S. A. Jaafar, and S. H. Mohamed, "Conventional Methods of Dissolved Gas Analysis Using Oil-Immersed Power Transformer for Fault Diagnosis: A Review," Electric Power Systems Research, vol. 216, p. 109064, 2023, doi: 10.1016/j.epsr.2022.109064.

[74] Y. Zhou et al., "Vibration Signal-Based Fusion Residual Attention Model for Power Transformer Fault Diagnosis," IEEE Sensors Journal, vol. 24, no. 10, pp. 17231–17242, 2024, doi:10.1109/JSEN.2024.3382811.

[75] C. M. Bishop, Pattern Recognition and Machine Learning. New York, NY, USA: Springer, 2006.

[76] K. P. Murphy, Machine Learning: A Probabilistic Perspective. Cambridge, MA, USA: MIT Press, 2012.

[77] S. Russell and P. Norvig, Artificial Intelligence: A Modern Approach, 4th ed. Hoboken, NJ, USA: Pearson, 2021.

[78] J. McCarthy, M. Minsky, N. Rochester, and C. E. Shannon, "A Proposal for the Dartmouth Summer Research Project on Artificial Intelligence," 1955.

[79] V. N. Vapnik, The Nature of Statistical Learning Theory. New York, NY, USA: Springer, 1995.

[80] T. M. Mitchell, Machine Learning. New York, NY, USA: McGraw-Hill, 1997.

[81] I. Goodfellow, Y. Bengio, and A. Courville, Deep Learning. Cambridge, MA, USA: MIT Press, 2016.

[82] S. Russell and P. Norvig, Artificial Intelligence: A Modern Approach, 4th ed. Hoboken, NJ, USA: Pearson, 2021.

[83] S. Shalev-Shwartz and S. Ben-David, Understanding Machine Learning: From Theory to Algorithms. Cambridge, U.K.: Cambridge University Press, 2014.

[84] I. Goodfellow, Y. Bengio, and A. Courville, Deep Learning. Cambridge, MA, USA: MIT Press, 2016.

References

[85] V. N. Vapnik, Statistical Learning Theory. New York, NY, USA: Wiley, 1998.

[86] T. Hastie, R. Tibshirani, and J. Friedman, The Elements of Statistical Learning: Data Mining, Inference, and Prediction, 2nd ed. New York, NY, USA: Springer, 2009.

[87] C. M. Bishop, Pattern Recognition and Machine Learning. New York, NY, USA: Springer, 2006.

[88] S. Shalev-Shwartz and S. Ben-David, Understanding Machine Learning: From Theory to Algorithms. Cambridge, U.K.: Cambridge University Press, 2014.

[89] K. P. Murphy, Machine Learning: A Probabilistic Perspective. Cambridge, MA, USA: MIT Press, 2012.

[90] T. Hastie, R. Tibshirani, and J. Friedman, The Elements of Statistical Learning: Data Mining, Inference, and Prediction, 2nd ed. New York, NY, USA: Springer, 2009.

[91] R. S. Sutton and A. G. Barto, Reinforcement Learning: An Introduction, 2nd ed. Cambridge, MA, USA: MIT Press, 2018.

[92] L. P. Kaelbling, M. L. Littman, and A. W. Moore, "Reinforcement Learning: A Survey," Journal of Artificial Intelligence Research, vol. 4, pp. 237–285, 1996.

[93] Author's illustration based on the literature review.

[94] I. Goodfellow, Y. Bengio, and A. Courville, Deep Learning. Cambridge, MA, USA: MIT Press, 2016.

[95] T. G. Dietterich, "Ensemble Methods in Machine Learning," in Multiple Classifier Systems, Berlin, Germany: Springer, 2000, pp. 1–15.

[96] Z.-H. Zhou, Ensemble Methods: Foundations and Algorithms. Boca Raton, FL, USA: CRC Press, 2012.

[97] A. Joshi, R. Khathoon, A. P. P. V., and V. Vinod, "A Very Fast and Easily Implementable Support Vector Machine Based Relay Algorithm to Classify the Fault and Non-Fault Disturbance in VSC HVDC Terminals," Electric Power Systems Research, vol. 220, p. 109380, 2023.

References

[98] M. Sheykhmousa, M. Mahdianpari, H. Ghanbari, F. Mohammadimanesh, P. Ghamisi, and S. Homayouni, "Support Vector Machine Versus Random Forest for Remote Sensing Image Classification: A Meta-Analysis and Systematic Review," IEEE Journal of Selected Topics in Applied Earth Observations and Remote Sensing, vol. 13, pp. 6308–6325, 2020.

[99] O. Kherif, Y. Benmahamed, M. Teguar, A. Boubakeur, and S. S. Ghoneim, "Accuracy Improvement of Power Transformer Faults Diagnostic Using KNN Classifier with Decision Tree Principle," IEEE Access, vol. 9, pp. 81693–81701, 2021.

[100] P.-N. Tan, M. Steinbach, and V. Kumar, Introduction to Data Mining, 2nd ed. Boston, MA, USA: Pearson, 2018.

[101] L. Lessa, C. Grilo, A. Moraes, D. Coury, and R. Fernandes, "A Travelling Wave-Based Fault Locator for Radial Distribution Systems Using Decision Trees to Mitigate Multiple Estimations," Electric Power Systems Research, vol. 223, p. 109646, 2023.

[102] J. R. Quinlan, C4.5: Programs for Machine Learning. San Francisco, CA, USA: Morgan Kaufmann Publishers, 1993.

[103] Y. Freund and R. E. Schapire, "A Decision-Theoretic Generalization of On-Line Learning and an Application to Boosting," Journal of Computer and System Sciences, vol. 55, no. 1, pp. 119–139, 1997.

[104] Y. Freund and R. E. Schapire, "A Decision-Theoretic Generalization of On-Line Learning and an Application to Boosting," Journal of Computer and System Sciences, vol. 55, no. 1, pp. 119–139, 1997.